Galileo Galilei
—GG—

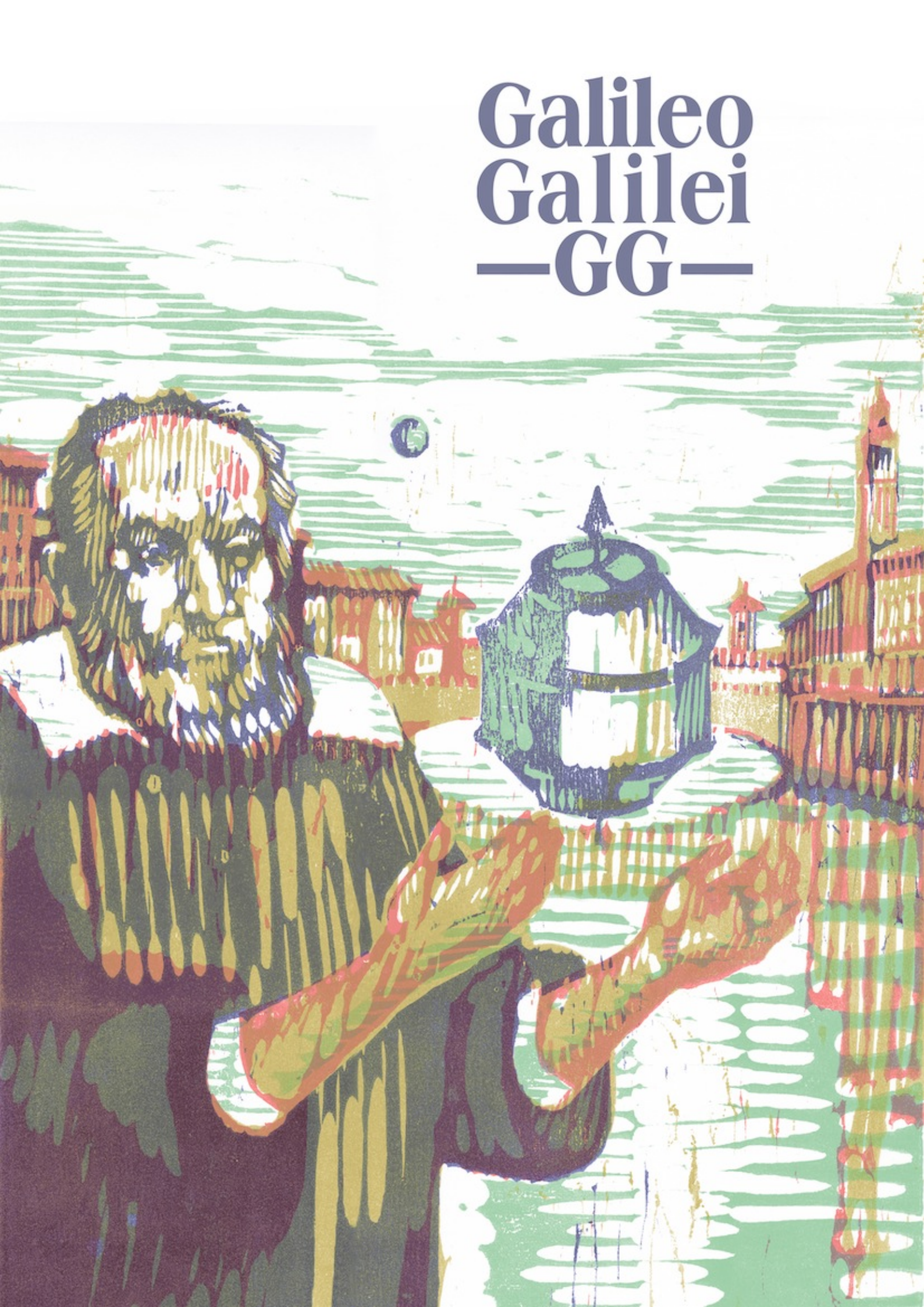

Galileo Galilei (GG): a small mission to test the weak equivalence principle of Galileo, Newton and Einstein to 10^{-17}

Submitted 15 June 2012 in response to ESA "Call for a small mission opportunity for launch in 2017"

Contact person: Anna M. Nobili, University of Pisa, Department of Physics "E. Fermi"
Largo Bruno Pontecorvo 3, 56127 Pisa, Italy; nobili@dm.unipi.it

Anna M. Nobili	University of Pisa and INFN, Italy
Michael Shao	Jet Propulsion Laboratory, USA
Raffaello Pegna	INFN, Italy
Slava Turyshev	Jet Propulsion Laboratory, USA
Georgi Dvali	CERN, Switzerland
Guido Zavattini	University of Ferrara and INFN, Italy
David M. Lucchesi	INAF- IAPS Roma and INFN, Italy
Andrea De Michele	University of Pisa, Italy
Robert Spero	Jet Propulsion Laboratory, USA
Paolo de Bernardis	University of Roma "La Sapienza," Italy
Valerio Iafolla	INAF- IAPS Roma, Italy
Federico Palmonari	University of Bologna and INFN, Italy
Joseph A. Burns	Cornell University, USA
Kim Aaron	Jet Propulsion Laboratory, USA
Rana Adhikari	Caltech, USA
Suresh Doravari	Caltech, USA
Michael Kramer	MPIfR Bonn, Germany
Juergen Mueller	IfE-Leibniz University Hannover, Germany
Norbert Wex	MPIfR Bonn, Germany
Reiner Rummel	TU Munchen, Germany
Harald Schuh	TU Wien, Austria
Johannes Boehn	TU Wien, Austria
Rudolf Dvorak	University of Vienna, Austria
Reza Tavakol	Queen Mary, University of London, UK
Joao Magueijo	Imperial College London, UK
Federico Ferrini	EGO Pisa, Italy
Francesco Pegoraro	University of Pisa, Italy
Angela Di Virgilio	INFN Pisa, Italy
Dino Leporini	University of Pisa, Italy
Carlo Bradaschia	INFN Pisa, Italy
Riccardo De Salvo	University of Sannio, Italy and University of Tokyo, Japan
Massimo Inguscio	LENS and University of Firenze, Italy
Guglielmo Tino	University of Firenze and INFN, Italy
Maria Luisa Chiofalo	University of Pisa, Italy
Giovanni Mengali	University of Pisa, Italy
Valeria Ferrari	University of Roma "La Sapienza," Italy
Sabino Matarrese	University of Padova, Italy
Paolo Molaro	INAF-OAT Trieste, Italy
Fernando De Felice	University of Padova, Italy
Silvia Masi	University of Roma "La Sapienza," Italy
Paolo Tortora	University of Ferrara, Italy
Maria Teresa Crosta	INAF-OATO Torino, Italy
Roberto Peron	INAF-IAPS Roma, Italy
Giuseppe Bertin	University of Milano, Italy
Andrea Ferrara	SNS Pisa, Italy
Enrico Iacopini	INFN Firenze, Italy
Angelo Scribano	INFN Pisa, Italy
Angelo Tartaglia	Politecnico di Torino, Italy
C. S. Unnikrishnan	TATA Institute, Mumbai, India
G. Rajalakshmi	TATA Institute, Mumbai, India
Christian Trenkel	ASTRIUM, UK
Alberto Anselmi	TAS-I Torino, Italy
Giuseppe Catastini	TAS-I Roma, Italy
Gianfranco Sechi	TAS-I Torino, Italy
Stefano Cesare	TAS-I Torino, Italy

Niuna impresa, pur minima che sia
può avere
Cominciamento o fine
senza queste
Tre Cose: Senza Sapere
senza Potere
Senza con amore Volere.

(anonimo fiorentino, 1300)

No matter how small an undertaking,
it cannot start or come to fruition
without knowledge,
without means,
or without loving tenacity.

(anonymous from Florence, 1300)

Cover and logo: color and black and white xylographies by Alice Milani Comparetti

Abstract (inserted online as required on proposal submission)

GG is a small mission with a first class science goal. It will test the Universality of Free Fall and the Weak Equivalence Principle to 1 part in 10^{17}. General Relativity is our best theory of gravity, but all attempts at merging gravity with the other forces of nature have failed and most of the mass of the universe is unexplained. General Relativity rests on the validity of the Universality of Free Fall. A confirmation would strongly constrain physical theories, whereas experimental evidence of violation would be revolutionary. With a huge leap by 4 orders of magnitude, GG will deeply probe a totally unexplored physical domain.

Thanks to its innovative sensor, GG's objective can be achieved at room temperature with a small spacecraft. A full scale ground prototype, GGG, which replicates many essential features of the space instrument, is operational in Pisa as a national INFN experiment. GGG will be used as a full scale prototype of the sensor to fly in GG and a test bed for its technologies.

The physical properties of the sensor are well established and allow the signal to be unambiguously distinguished from systematic errors. A full error analysis is available, based on experimental measurements and an end-to-end software simulator. The error budget shows the measurement objective can be reached in 1 day integration time, the rest of the mission being devoted to improving the accuracy and performing checks against systematic errors.

The orbit is a standard near circular low altitude ($\simeq 600$ km) sun synchronous dawn-dusk orbit. The mission duration is 9 months and it includes three measurement intervals separated by spin axis correction maneuvers.

The GG sensor is a differential accelerometer with two concentric, heavy (10 kg) test cylinders made from different materials, Be and Ti, weakly coupled in 2D, co-rotating with the spacecraft at 1 Hz. Fast rotation provides up-conversion of the signal to high frequency without attenuation, reduced thermal noise, auto-centering. The coupling is by thin U-shape flexures fully tested in the lab. The read-out is capacitive as in the GGG lab prototype and will be replaced by a laser interferometry gauge with JPL participation. The sensor is enclosed within the weakly suspended PGB lab, which screens the sensor from various disturbances and mounts instrumentation.

The GG spacecraft is passively stabilized by 1-axis rotation at 1 Hz. The only high tech feature is drag free control at orbital frequency, the algorithms of which are available as fully tested software routines. It uses cap sensors as in the lab prototype and cold gas micro-thrusters actuators as qualified for GAIA. With 400 kg total mass, 1.4 m width and 1.2 m height it fits as a piggyback passenger of VEGA.

GG fits a 4-year implementation schedule, from Phase B to launch. At system level, a Proto Flight Model approach is envisaged. All platform equipment have flight heritage or are derived from equipment with flight heritage, with one exception, the spin rate sensor, a prototype of which was designed and breadboarded in 2009. As for the payload, neither mechanics nor electronics require substantial technology development, given the experience from GGG. Development models are envisaged for the 0-g flexures, the wireless data transmission and the lock mechanisms.

In the past GG was studied by the Italian space agency (ASI). The latest study, Phase A-2, was completed in 2009 and included an official cost estimate for a 4-yr development. We have updated that cost estimate for the present proposal, adding launch and ground segment costs omitted in 2009. Given this heritage, a sharing of responsibilities is proposed with ASI acting as mission architect and providing the science payload and operations, and ESA acting as spacecraft architect and procuring the spacecraft platform and the launcher. ASI will also coordinate the participation from institutes interested in collaboration, including NASA-JPL.

Executive summary

General Relativity (GR) is the best theory of gravity to-date. It governs physics at the macroscopic and cosmic scales and it has been highly successful in the confrontation with experiments [1]. However, all attempts at merging gravity with the other forces of nature have failed and most of the mass of the universe is unexplained.

In Einstein's own words [2] GR rests on an experimental fact proven to very good precision: that in a gravitational field all bodies are equally accelerated regardless of their mass and composition (*Universality of Free Fall-UFF*). UFF comes from Newton's equations in the assumption that inertial and gravitational mass are equivalent (*Weak Equivalence Principle-WEP*). In 1907 [3], based on UFF, Einstein derived the more general *Einstein Equivalence Principle-EEP* from which 9 years later he formulated GR [4]. Should experiments invalidate UFF/WEP, either GR must be amended, as it happened to Newton's gravity, or we are in the presence of a new so far unknown physical interaction. Either way, it would be a scientific revolution. This is why UFF/WEP tests must be pushed to the highest possible precision whenever the possibility arises.

A huge leap took place in the early 1900 when Eötvös had the innovative idea to place the proof masses on a balance and suspend its center of mass from a thin wire. The torsion balance is almost a miraculous instrument for testing UFF: the center of mass aligns itself with local gravity, hence any force which is the same on both masses is perfectly rejected (common mode effects cause no deflection). Only differential effects, such as a deviation from UFF, cause a torque and deflect the wire: no violation, no torque, no signal. Experiments of this kind are *null experiments*. They are among the highest precision physics experiments one can think of. In addition, the torsion balance is extremely sensitive: with a very thin fiber even the tiniest torque gives a deflection that a good read-out can detect. Eötvös proved UFF/WEP to $\simeq 10^{-8}$ [5], a result not matched for half a century. Einstein regarded it as the "green light" for GR since it made the foundations of the theory extremely robust ([4], p. 114).

With the space age time came for GR to be challenged by experiments. Could Eötvös tests be further improved? Did they have any Achille's heel? Indeed, they lacked modulation, because a violation signal from the Earth is DC. In the 1960-70s Dicke and Braginsky found a solution. If the data of the balance are analyzed for violation in the field of the Sun rather than the Earth, then diurnal rotation modulates the signal with no need to spin the balance, which everybody feared because of rotation noise. This simple way of modulating the signal allowed them to gain 3 to 4 orders of magnitude. They proved no violation to 10^{-11} [6] and 10^{-12} [7].

Physicists know that up-converting low frequency signals to higher frequency (the higher the better) is very effective in reducing noise. Diurnal frequency is very low and diurnal noise on Earth is everywhere. If modulation occurs by rotation, can the balance be spun faster than the Earth with sufficiently low rotation noise? In the last 20 years the Eöt-Wash group has developed sophisticated techniques to slowly rotate torsion balances. They have confirmed no violation in the field of the Sun to 10^{-12} [8] and proved no violation in the field of the Earth to 10^{-13} [9].

The success of the torsion balance is astonishing if we note that its masses *fall* with an acceleration 600 to 1800 times smaller (depending on the source body being the Earth or the Sun) than that of free falling bodies in mass dropping tests. That is, on paper, the latter should be 3 orders of magnitude more sensitive simply because of their stronger signal. Instead, torsion balances have superseded mass dropping tests by far. For 3 main reasons: mass dropping tests are not null experiments; they are plagued by release errors (unless the masses are released with exactly the the same position and velocity they fall differently and therefore mimic a violation); the experiment duration is too short.

Tests based on dropping cold atoms are many orders of magnitude less sensitive than those with macroscopic bodies. They have reached 10^{-7} with atom species differing by 2 neutrons only [10] while the gravitational acceleration g has been measured to $3 \cdot 10^{-9}$ with a single species of cold atoms [11].

Aside from laboratory controlled experiments, laser ranging to the Moon has shown that the

Earth and the Moon fall with the same acceleration in the field of the Sun to 10^{-13} [12], [13].

Torsion balances have been pushed to their thermal noise limit ([14], Fig. 20). Lunar laser ranging technology and physical modeling are being improved [15], but there are fundamental limitations [16]. Both experiments have come close to their limits. There may still be room for some improvement, but a leap forward by several orders of magnitude as it happened with Eötvös and then with Dicke and Braginski is extremely unlikely. We argue that a 4 orders of magnitude leap, to reach 10^{-17}, can happen in space with GG because of its innovative design. With such a deep probing of an unexplored physical domain even evidence of no violation would tightly constrain physical theories for decades.

By orbiting the Earth at low altitude a torsion balance gains 3 orders of magnitude in the strength of the signal. However, at zero-g it loses its perfect common mode rejection. Moreover, in space proof masses should be concentric to reduce gravity gradients (tides). The GG sensor is the balance for space. Two concentric test cylinders weakly coupled as a 2D mechanical oscillator spin along the symmetry axis much faster than their natural frequency, up-converting the signal to more than 3 orders of magnitude higher frequency than ever achieved while also auto-centering on each other very precisely by physical laws. Mechanical, electronic and thermal noise competing with the signal are drastically reduced and no signal attenuation occurs, making cryogenics unnecessary [17]. Motor and bearings are not needed. A sensitivity close to that of a high quality torsion fiber is possible with very weak laminar suspensions because of weightlessness. Very good rejection of common mode forces is possible (by 10^{-5}) because the GG sensor is in essence a beam balance whose arms can be adjusted against air drag. On ground, against a force 50 million times stronger, beam balances have reached a rejection of $5 \cdot 10^{-10}$ [18]. A full scale GG prototype on ground (GGG) has the same number of degrees of freedom, the same dynamical features of the instrument to fly and provides experimental results directly relevant to GG. GGG is an approved national experiment of INFN. Cylindrical symmetry and rapid rotation of the sensor (@ 1Hz) drive the GG spacecraft to be a classic spacecraft passively stabilized by 1-axis rotation, with weak coupling to the co-rotating payload to ensure nutation damping. The only modern technology required is drag compensation around the orbital frequency by cold gas microthrusters, the algorithms of which are available as fully tested software routines on heritage from GOCE. Thus, most of the critical issues are addressed by design without the need of brute force approaches, such as operating in cryogenics conditions.

The advantage of GG is apparent by comparison with the thermal noise of μSCOPE, which aims at 10^{-15} ([19], Table 5). Should μSCOPE aim at 10^{-17} like GG, at room temperature, it would need an integration time of $\simeq 39\,\mathrm{yr}$ [20], while GG has an integration of time of a few hours and plans to perform a full test to 10^{-17} in 1 day [21]. μSCOPE was to fly in 2004 [22], now postponed to 2016. Whatever the result, GG will check it with 100 times better precision. Only STEP aimed at 10^{-17} like GG; it required cryogenics and was studied by ESA (twice) as a medium size mission [23], [24]. It was later proposed to NASA with a 10 times higher precision goal.

In 1960 Schiff [25] demonstrated that a measurement of the gravitational redshift is a test of UFF/WEP, and showed that at as such it was not competitive with Eötvös type tests. Since then clocks have considerably improved but measurements of the gravitational redshift are still not competitive by far [26].

GG is a small satellite (400 kg) to be injected in a $\simeq 600\,\mathrm{km}$ altitude near circular standard sun-synchronous Earth orbit for a 9-month duration. It fits as a piggy back inside a full VESPA adapter of VEGA. In the past GG was studied by the Italian space agency (ASI). The latest study, Phase A-2, was completed in 2009 and included an official cost estimate for a 4-yr development from Phase B to launch. We have updated that cost estimate for the present proposal, adding launch and ground segment costs omitted in 2009. Given this heritage, a sharing of responsibilities is proposed with ASI acting as mission architect and providing the science payload and operations, and ESA acting as spacecraft architect and procuring the spacecraft platform and the launcher. ASI will also coordinate the participation from institutes interested in collaboration, including NASA-JPL.

Contents

GG Acronym and Symbols

Acronym	Name	Acronym	Name
AIT	Assembly Integration and Testing	PCU	Power Control Unit
AOM	Acoustic Optic Modulators	PDR	Preliminary Design Review
ASI	Agenzia Spaziale Italiana	PFM	Protoflight Model
AOCS	Attitude and Orbit Control Subsystem		
ATB	Avionics Test Bench	PGB	Pico Gravity Box
BU	Business Units	PSD	Position Sensing Detector
CBE	Current Best Estimate		
C/D		ROM	Rough Order of Magnitude
CDMU	Command and Data Management Unit	s/c	Spacecraft
CDR	Critical Design Review	SEP, EEP	Strong Equivalence Principle, Einstein Equivalence Principle
CMR	Common Mode Rejection	SIM	Space Interferometry Mission
CPE	Control & Processing Electronics	SOC	Science Operations Centre
DA	Differential accelerometer		
DC	Direct Current	S/S	Subsystem
DFACS	Drag Free & Attitude Control Subsystem	SSO	Sun Synchronous Orbit
DFC	Drag Free Control	STEP	Satellite Test of the Equivalence Principle
ECE	Experiment Control Electronics	STM	Structural-Thermal Model
EEP	Einstein Equivalence Principle	SW	Software
EMC	Electromagnetic Compatibility	TAS-I	Thales Alenia Space Italia
EP	Equivalence Principle	TB	Test Bench
ESA	European Space Agency	TBC	To Be Confirmed
FAR	Flight Acceptance Review	TES	Tropospheric Emission Spectrometer
FDIR	Failure Detection, Isolation and Recovery	TM	Test Mass
FEEP	Field Emission Electric Propulsion	TT &C	
FFT	Fast Fourier Transform	TRL	Technology Readiness Level
FM	Flight Model	TRR	Test Readiness Review
GAIA	ESA Astrometry and Fundamental Physics Mission soon to be launched	TV	Thermal Vacuum
GG	Galileo Galilei (Satellite)	UFF	Universality of Free Fall
GGG	Galileo Galilei on the Ground (Experiment)	VEGA	Vettore Europeo di Generazione Avanzata
GOCE	Gravity and Ocean Circulation Explorer	VESPA	VEga Secondary Payload Adapter
GR	General Relativity	WEP	Weak Equivalence Principle
GSE	Ground Support Equipment	μSCOPE	Micro-Satellite à traînée Compensée pour l'Observation du Principe d'Equivalence
HW	Hardware	pm	picometer
		$\eta = \frac{\Delta a}{a}$	fractional differential acceleration of the free falling test masses.
INFN	Istituto Nazionale di Fisica Nucleare	ν_{spin}	s/c spin frequency w.r.t. LVLH Reference Frame
IRF	Inertial Reference Frame	P_{spin}	s/c spin period
IU	Industrial Units	ν_{orb}	s/c orbital frequency w.r.t. IRF
I/F	Interface	P_{orb}	s/c orbital period
I&T	Integration & Testing	ν_{DM}	natural frequency of proof masses differential oscillation.
JPL	Jet Propulsion Laboratory	P_{DM}	natural period of proof masses differential oscillation.
LG	laser gauge	ν_{PGB}	PGB natural oscillation frequency in sensitivity plane.
LGA	Low Gain Antenna	P_{PGB}	PGB natural oscillation period in sensitivity plane.
LGE	Laser Gauge Electronics	ν_{CM}	test masses Common Mode oscillation frequency in the sensitivity plane
LOLA	Lunar Orbiter Laser Altimeter	P_{CM}	test masses Common Mode oscillation period in the sensitivity plane
LVLH	Local Vertical Local Horizontal	ν_{PGBz}	PGB natural oscillation frequency along spin axis.
LRR	Launch Readiness Review	P_{PGBz}	PGB natural oscillation period along spin axis.
MBW	Measurement Bandwidth	ν_z	test masses Common Mode oscillation frequency along spin axis.
MOC	Mission Operations Centre	P_z	test masses Common Mode oscillation period along spin axis.
MSL	Mars Science Laboratory	T_{int}	integration time
NASA	National Aeronautics and Space Administration		
PCDU	Power Control and Distribution Unit		

1 Introduction: GG fact sheet

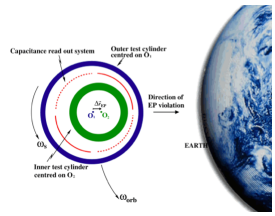

GG will test the Universality of Free Fall and the Weak Equivalence Principle on which General Relativity relies to 1 part in 10^{17} improving current best results by 4 orders of magnitude. Thanks to an innovative sensor the task can be achieved at room temperature with a small spacecraft in a sun synchronous low Earth orbit. The physical properties of the sensor are well established [17] and allow the signal to be distinguished from systematics unambiguously .

A full scale ground prototype which replicates many essential features of the space experiment is operational in Pisa as a national INFN experiment.

GG has been the subject of in depth studies by the Italian space agency (ASI). The latest one at Phase A-2 level was completed in 2009 and included an official cost estimate for a 4-yr development, from start of Phase B to launch. We have updated it for the present proposal.

GG is a small mission with first class science goal.

The science case

General Relativity is the best theory of gravity to-date. However, all attempts at merging gravity with the other forces of nature have failed and most of the mass of the universe is unexplained.

General Relativity rests on the validity of the Universality of Free Fall and the Weak Equivalence Principle.

Experimental evidence of violation would be revolutionary because either General Relativity is incorrect or we are in the presence of a new physical interaction. A confirmation would strongly constrain physical theories.

With a huge leap by 4 orders of magnitude GG will deeply probe a totally unexplored physical domain.

The spacecraft and the mission

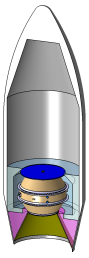

The GG s/c is passively stabilized by 1-axis rotation at 1 Hz. The only high tech feature is drag free control at orbital frequency, which has been designed during GG Phase A-2 Study in 2009 based on GOCE expertise. It uses cap sensors as in the GGG lab prototype and cold gas micro-thrusters actuators as qualified for GAIA.

With 400 kg total mass, 1.4 m width and 1.2 m height it fits inside a (full) VESPA piggy back adapter of VEGA.

The orbit is a standard, near circular, low altitude ($\simeq$ 600 km) sun synchronous orbit with no special launch requirements. The mission duration is 9 months.

The payload

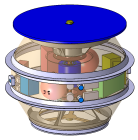

At the heart of the s/c is the GG sensor: a differential accelerometer with 2 concentric test cylinders made of different material, 10 kg each, weakly coupled in 2D co-rotating with the s/c at 1 Hz. It provides: up-conversion of the signal to high frequency without attenuation, reduced thermal noise, auto-centering [17]. It is a balance in space.

The coupling is by thin U-shaped flexures fully tested in the lab. The read out is capacitive as in GGG, to be replaced by a laser interferometry gauge with JPL-NASA participation.

The sensor is enclosed by the weakly suspended PGB lab. It screens the sensor from various disturbances and mounts instrumentation.

GGG: GG on Ground prototype

GGG is a full scale prototype of the sensor to fly in GG, with the same number of degrees of freedom and the same dynamical features. It is less sensitive than in space due to the stiffer coupling needed at 1-g, but it is operated like in space.
It is limited by terrain and bearings tilt noise on the suspension shaft, both absent in space.

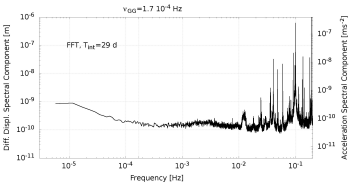

With a very effective passive attenuation and 29 d integration time GGG has measured $1.8 \cdot 10^{-10}$ m displacement @ the GG signal frequency $\nu_{orb} = 1.7 \cdot 10^{-4}$ Hz, while the target in space is 300 times smaller. Further noise attenuation and weaker suspensions have been designed and are going to be implemented.

2 Scientific objectives and requirements

2.1 GG science goal

The goal of GG is to test the Universality of Free Fall (UFF) to a precision of 1 part on 10^{17} in the measurement –at room temperature– of the fractional differential acceleration $\eta = \Delta a/a$ between two proof masses made of Be and Ti weakly suspended inside a 1 Hz spin-axis stabilized spacecraft orbiting the Earth in a $\simeq 600$ km altitude near circular sun-synchronous orbit. This would improve current best results by 4 orders of magnitude [9] [12] [13]. The relevance of this goal is well known within ESA science directorate, since a medium size cryogenic M-level mission aiming at the same target was studied twice, first in collaboration with NASA [23] and by ESA alone [24] .

General Relativity (GR) rests on the fact that UFF holds. In [27] (p. 364) reference is made to a manuscript written by Einstein in 1919 which reads: "When, in the year 1907, I was working on a summary essay concerning the special theory of relativity for the Jahrbuch fuer Radioaktivitaet und Elektronik, I had to try to modify Newton's theory of gravitation in such a way that it would fit into the theory. Attempts in this direction showed the possibility of carrying out this enterprise, but they did not satisfy me because they had to be supported by hypotheses without physical basis. At that point, there came to me the happiest thought of my life, in the following form:

Just as is the case with the electric field produced by electromagnetic induction, the gravitational field has similarly only a relative existence. *For if one considers an observer in free fall, e.g. from the roof of a house, there exists for him during his fall no gravitational field –at least in his immediate vicinity.*"

Einstein recalled the same facts in a speech given in Kyoto in 1922 entitled "How I created the theory of relativity" [2]: "While I was writing this, I came to realize that all the natural laws except the law of gravity could be discussed within the framework of the special theory of relativity. I wanted to find out the reason for this, but I could not attain this goal easily.

. . . The breakthrough came suddenly one day. I was sitting on a chair in my patent office in Bern. Suddenly a thought struck me: If a man falls freely, he would not feel his weight. I was taken aback. This simple thought experiment made a big impression on me. This led me to the theory of gravity. I continued my thought: A falling man is accelerated. Then what he feels and judges is happening in the accelerated frame of reference. I decided to extend the theory of relativity to the reference frame with acceleration. I felt that in so doing I could solve the problem of gravity at the same time.

. . . It took me eight more years until I finally obtained the complete solution."

Thus, the well tested UFF leads to the statement that a (uniform) gravitational field and an accelerated frame (with uniform linear acceleration equal and opposite to the gravitational acceleration) are equivalent with respect to all physical processes. The equivalence of systems with uniform linear velocity relative to each other is thus extended to the equivalence of systems with uniform linear acceleration relative to each other. This is a crucial leap from Newton's equivalence between inertial and gravitational mass (destined to become the Weak Equivalence Principle-WEP) to the Strong Equivalence Principle-SEP (also referred to as Einstein Equivalence Principle-EEP). SEP relies on WEP, which is the same as UFF: ultimately, if UFF is invalidated by experiments so is the SEP.

In summary, GR is founded on SEP, which in its turn relies on WEP, which is the same as UFF: if UFF is invalidated by experiments, so is the SEP. In such case, either GR should be amended because it is not a fully correct theory of gravity or else we would be in the presence of a new, so far unknown, physical interaction. UFF experiments test a fundamental physical principle; moreover, they can reach extremely high accuracy because they can be performed as *null experiments*. This is why they are extremely powerful probes of fundamental physics worth improving whenever possible.

In 1916 the best experimental tests of UFF/WEP were those by Eötvös [5], which had started in the 1889 and Einstein explicitly recognized their relevance ([4],§ 2): "...This view is made possible for us by the teaching of experience as to the existence of a field of force, namely the

gravitational field, which possesses the remarkable property of imparting the same acceleration to all bodies* (Footnote: *Eötvös has proved experimentally that the gravitational field has this property in great accuracy)."

With a huge leap by 4 orders of magnitude GG will deeply probe a totally unknown physical domain. Confirmation would strongly constrain theories for decades. Evidence of a violation would be revolutionary.

2.2 Why GG?

At present slowly rotating torsion balances have reached the level of thermal noise [14] and LLR tests [15] are also close to their limits [16]. One order of magnitude might still be gained, but an improvement by 4 orders of magnitude is beyond reach for both these experiments.

The next leap requires a torsion balance type of instrument in low orbit around the Earth, where the driving signal (the gravitational acceleration from the Earth) is about 3 orders of magnitude stronger than on ground balances, absence of weight allows very weak coupling of the test masses (hence high sensitivity), and the signal can be modulated at very high frequency with no need for motor and bearings if the s/c is spin-axis stabilized. However, a torsion balance is not suitable for space, and indeed it was never proposed.

Tests based on dropping cold atoms are many orders of magnitude less sensitive than those with macroscopic bodies. They have reached 10^{-7} with atom species differing by 2 neutrons only [10], which makes the case for a possible violation very weak. Being mass dropping tests they do not take advantage of a stronger signal in space (the Earth's gravitational acceleration is in fact slightly smaller at low Earth orbit than on ground) and the advantage of a slightly longer interrogation time may not be worth the effort of an experiment in space. As for the measurement of the gravitational redshift, in 1960 Schiff [25] demonstrated that it is a test of UFF/WEP, and showed that at as such it was not competitive with Eötvös type tests. Since then clocks have considerably improved but measurements of the gravitational redshift are still not competitive by far [26].

The GG sensor is a balance for space, designed to exploit all advantages of space(Fig. 1). It is a mechanical oscillator in which two concentric test masses (coaxial cylinders) are very weakly coupled in 2D, to ensure high sensitivity to differential forces acting in the sensitive plane, while rapidly rotating around the symmetry axis perpendicular to it (Fig. 1, center). This is by definition a *supercritical* rotor, meaning that the spin rate is higher (indeed much higher) than the natural coupling frequency of the test masses. In GG rotation is provided by the s/c with 1 s spin period, while the test cylinders (10 kg each) are coupled with $\simeq$ 540 s natural differential period. It is known that in such system: i) the masses self-center at an equilibrium position defined by physical laws; ii) a force acting at a frequency higher than the natural one is not attenuated. Both properties depend crucially on the oscillator being sensitive in 2D. In 1D there is no stable equilibrium position and a signal at frequency higher than the natural one is attenuated as the ratio of the frequencies squared. The violation signal points to the center of mass of the Earth, hence it is at the satellite orbital frequency $\nu_{orb} \simeq 1.7 \cdot 10^{-4}$ Hz. The s/c rotation up-converts it to a frequency more than 3 orders of magnitude higher than ever achieved, with no reduction in strength. At that frequency thermal noise from internal damping is drastically lower than it is at ν_{orb} [17].

This fact makes all the difference because with a total integration time of about 3 hr required to reach signal-to-noise ratio of 2 [21] a full reliable measurement to the 10^{-17} target can be performed in 1 day only. The estimate includes thermal noise from gas damping and eddy currents.

Such a short integration time can be appreciated by comparison with μSCOPE, which aims at a test 100 times less accurate than GG, also at room temperature but with a 1D sensor. According to the PI [19], μSCOPE is expected to be limited by thermal noise due internal damping in the gold wire of 5 μm diameter and 2.5 cm length which connects the test masses to the instrument cages. The signal is up-coverted to the (low) frequency $\simeq 8 \cdot 10^{-4}$ Hz at which thermal noise is estimated to amount to $1.4 \cdot 10^{-12}\,\mathrm{ms}^{-2}/\sqrt{\mathrm{Hz}}$ ([19], Table 5). With the target $\eta_{\mu scope} = 10^{-15}$ and for a signal-to-noise ratio SNR = 2 the required integration time is $\simeq$ 1.4 d, i.e. the mission goal can be reached in 20.8 orbits of the satellite. Should μSCOPE aim at 10^{-17} like GG it would

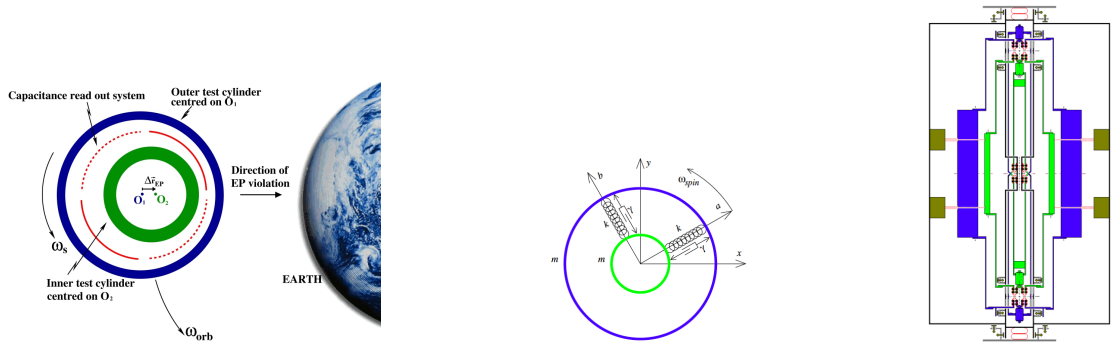

Figure 1: The GG sensor made of 2 coaxial concentric test cylinders (in green and blue) spinning around the symmetry axis and weakly coupled in the plane perpendicular to it. *Left*: the test cylinders (sensitive plane) in orbit around the Earth showing a violation signal pointing to the center of mass of the Earth and the capacitance sensors between them modulating the signal at the spin frequency. *Center*: the test cylinders weakly coupled as a 2D rotating mechanical oscillator. *Right*: section along the spin axis of the GG sensor/balance. Connection of the balance to the s/c outer shell is through an intermediate stage (the PGB and its shaft) to which the balance is connected at the center by means of U-shape weak lamellae (in red). This is the pivot of the balance. At its 2 ends each test cylinder is connected (through a light rigid interface and 3 U-shape lamellae 120° apart; 2 shown in planar section) to the 2 ends of the coupling arms; the short ones for the inner green cylinder; the long ones for the outer blue cylinder. The result is 2 spherical joints (see the red U-shape lamellae at the top and bottom). Any differential force acting between the test cylinders in the plane perpendicular to the symmetry axis will displace their centers of mass by tilting the coupling arms (pivoted at the center). Here the read out is shown not with capacitive sensors but with a laser gauge (laser boxes are fixed on the PGB and shown in brown; there are 3 of them, 120^o apart, above and below the symmetry plane of the test cylinders). At each end of the coupling arms (in blue and green) are shown the inch-worms which allow the balance to be balanced in order to reject accelerations acting in common mode on both cylinders. The two shorter parts of each coupling arm (pertaining to the inner cylinder and shown in green) have a small additional mass each (in green) so that the pivot center is at their center of mass. In the balance the mass of the test cylinders dominates over the mass of the coupling arms and interfaces. Note the sensor symmetry both in azimuth and top/down.

require a 10^4 times longer integration time (about 39 yr) which is obviously unfeasible. μSCOPE was to fly in 2004 [22], but it has recently been postponed to 2016. Whatever the result, GG will check it with 100 times better precision. Only STEP aimed at 10^{-17} like GG, but it required cryogenics which added in complexity and cost. It was studied by ESA (twice) as a medium size mission [23], [24]. It was later proposed to NASA with a 10 times higher precision goal.

GG very short integration time has a major impact on the payload and the overall complexity and cost of the mission because it avoids the need for an additional sensor with test masses made of the same material for zero check purposes. This has been known to be an issue, because the s/c has only one center of mass and disturbances may be different. Indeed, even with co-centered sensors (which would be possible in GG, and were investigated in the past) the sensors would inevitably be different, hence affected by different errors.

GG does not need an additional sensor because due to the very short integration time it can perform a systematic series of *null checks*. GG null checks rely on the following facts: 1) the EP violation target signal as well as the competing effects, all depend on the inclination angle θ_n between the spin axis and the orbit normal, but each one in its own way; 2) the spin axis of GG is fixed in inertial space (due to the rapid spin and high spin energy); 3) the orbit plane precesses about the North celestial pole at about 1°/d. In the GG mission plan there are 3 cycles of 76 d each devoted to science measurement. In 76 d θ_n varies from -38^o to $+38^o$ (only 2 attitude maneuvers are required). We therefore have 3 measurement cycles free from any maneuver and during each cycle a wide variation $-38^o < \theta_n < +38^o$ occurs.

Consider the most dangerous systematic error source, due to the coupling of the Earth's monopole with the quadrupole mass moments of the test cylinders. It has the same frequency and phase of the signal but its dependence on θ_n in this range shows (in the frequency domain) that it gives rise to a differential acceleration between the TMs not only at the orbital frequency

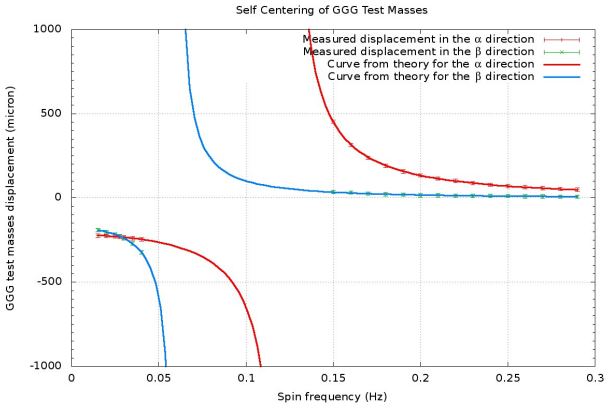

Figure 2: Experimental evidence of self centering of the test masses in the GGG prototype. The plot reports the relative displacements of the GGG test cylinders (10 kg, as designed in GG) due to rotation in the α and β directions fixed on the rotor. The centers of mass are initially displaced by $\varepsilon_\alpha \simeq -220$ μm and $\varepsilon_\beta \simeq -180$ μm in the α and β directions. Centrifugal forces due to rotation in subcritical regime (i.e. at rotation frequencies smaller than the natural frequencies $\nu_\alpha = 0.123$ Hz and $\nu_\beta = 0.06$ Hz) tend to increase the displacements, while in supercritical regime the test masses displacements go to the opposite direction and are reduced by the factor $\nu^2_{\alpha,\beta}/(\nu^2_{spin} - \nu^2_{\alpha,\beta})$ in perfect agreement with the theory of supercritical rotors.

(like the signal) but also at its 3rd harmonic. So, from the quadrupole coupling effect at 3 times the orbit frequency we can establish with certainty how much is its contribution at the orbit (signal) frequency which therefore must not be attributed to EP violation. Similarly, Earth's tidal effects will have, in addition to their effect at twice the orbit/signal frequency also an effect at 4 times this frequency.

As θ_n varies, also the effect of residual air drag can be distinguished from the signal, because the cross section of the satellite (hence its area-to-mass ratio to which the drag acceleration is proportional) changes with θ_n in a completely different way from the target signal. Similar null checks can be performed for the magnetic effects (though they are less important because they do not occur at the signal frequency) since their dependence on inclination is perfectly known.

By limiting null checks to offline data analysis only we reduce the complexity of the mission (1 single accelerometer), reduce risk and cost. They are very powerful and strong checks of the measured signal which allow us to establish beyond question whether the effect measured at orbital frequency and pointing to the Earth is to be attributed to a classical perturbing effect or to UFF/WEP violation and evidence of new physics.

Last but not least, the GG design allows a full scale GG on Ground (GGG) replica at 1-g. Fig. 3 reports the results of a 29 d run interrupted by the earthquake on 25 January 2012 with no damage to the 2D joints which suspend the test cylinders. The joints have however been damaged by the more recent earthquake at the end of May.

2.3 GG measurement procedure

Drag on GG due to residual atmosphere along its orbit is 50 million times smaller than 1-g, but it is also 2.5 billion times bigger than the target signal. Its effect is an inertial force on the suspended test masses which ideally should act the same on both of them (common mode effect). In reality it is not so; a good strategy is to partially compensate and partially reject it. A drag free control for GG has been developed in 2009 by TAS-I (Torino) based on GOCE expertise.

In order to reject common mode forces the concentric cylinders are arranged to form a peculiar beam balance (Fig. 1). The common mode force against which balancing is performed is the inertial force resulting from air drag on the spacecraft. On ground beam balances are balanced to $5 \cdot 10^{-10}$ [18] against 1-g; in GG the force to be balanced is 50 million times smaller than 1-g and therefore a good common mode rejection is expected. The mechanical suspensions are very

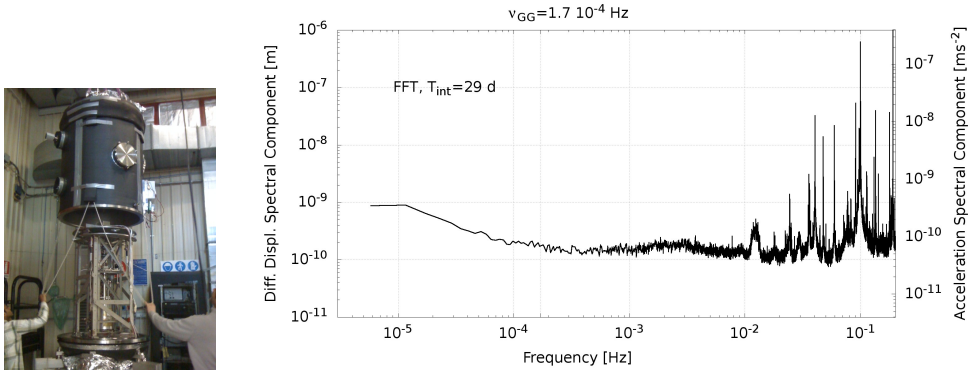

Figure 3: *Left:* the GGG protoype in Pisa. *Right:* FFT of the relative dispalcements of and differential accelerations the test cylinders in the horizontal plane of the lab measured in a 29 d run. At the frequency $1.7 \cdot 10^{-4}$ Hz of the signal in space we have measured a differential dispalcement of 180 pm, which is 300 times larger than what GG should detect in space. The limiting factors are terrain and bearings tilt noise on the shaft, both absent in space. They can, and will, be further reduced.

weak U-shape lamellae (a 10 kg proof mass inside GG requires a suspension that one would use on ground for suspending 0.2 milligram against local gravity). They provide also passive electric discharging of the test masses –which is crucial in gravity experiments– but unlike dummy wires they couple the masses in a well designed manner and ensure a small value of the relevant losses.

The displacements between the centers of mass of the test cylinders are read in the sensitive plane are read by 2 orthogonal co-rotating capacitance bridges, one of which is shown in Fig. 4. If the plates of each bridge are perfectly centered in between the test cylinders the measurement is unaffected by their displacements in common mode. For the measurement of the target differential signal $\Delta x_{EP} \simeq 0.6$ pm not to affected by common mode displacements the requirement on the bridge mevahnical balancing χ_{bridge} must be met.

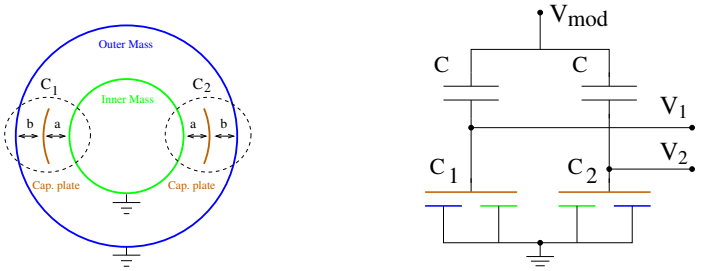

Figure 4: GG main capacitive bridge mechanical components (left) and Weastone bridge schematics (right). Each capacitor is formed by two surfaces, one for each of the two grounded bodies, and one plate, to which the sinusoidal voltage V_{mod} is applied. The other two capacitors of the bridge are the fixed capacitors C. Any displacement of the test masses with respect to the plates causes a loss of balance of the bridge and therefore the output signal $V_2 - V_1 \simeq \frac{V_{mod}}{4} \frac{C_1 - C_2}{C}$.

The calibration factor to be applied to the bridge measurements depends on the amplification factor of the readout electronics and on the sensitivity, that is on the mechanical dimensions, of the sensor. The readout electronics can be accurately tested and its gain precisely measured before launch; the capacitive sensor dimensions can be measured within a few micrometers. This allows the calculation of the capacitive bridge sensitivity within an error of a few parts in 10^4. The capacitive diplacement sensor in its final configuration can be tested on ground with its electronics by appropriately holding and displacing the test masses while acquiring data from the readout; this also allows to test and initially adjust the capacitive bridge centering.

The output data received from the GG experiment in space will be the relative displacements of the test cylinders in 2 orthogonal directions α, β of the sensitive plane of the GG accelerometer

(perpendicular to the spin/symmetry axis). These will be in the form of two time series α_i, β_i with a given sampling time $\tau_{sampl} = T_{spin}/2^n$, 2^n being the number of data points recorded per spin period T_{spin}. For instance, in the GGG prototype we have $2^5 = 32$ data points per spin period, hence two subsequent data points are separated by the sampling time $T_{spin}/32$). For each data point α_i, β_i we will also receive the phase angle φ_i of the rotating test cylinders; in GGG a rotary encoder associates to each data point its specific angular position relative to a fixed direction in the non rotating system.

Let us consider the GG satellite in its sun-synchronous orbit assuming, for the sake of discussion, zero eccentricity and spin axis perpendicular to the orbit plane. Figure 5 shows a sketch of the satellite on its orbit and defines the so called *Local Vertical Local Horizontal (LVLH)* reference frame with axes $x_{LVLH}, y_{LVLH}, z_{LVLH}$ as shown. The z_{LVLH} axis is directed along the spin axis, i.e. it is parallel to the spin angular velocity vector, but it is not spinning. In the LVLH frame a violation signal is a constant (DC) vector directed along the x_{LVLH} axis, i.e. along the *GG–Center of mass of the Earth* direction. If the phase φ_i of the output data is measured from the x_{LVLH} axis —which means that the spin frequency is referred to the center of the Earth (we call it $\nu^{\oplus}_{spin}$)— the FFT of the time series α_i, β_i will show –in case of violation– a peak at $\nu^{\oplus}_{spin}$ above random noise (assuming that all systematics –like air drag– have been reduced below the EP violation effect). If we demodulate to the non rotating LVLH reference frame –using the phase time series φ_i– both the signal and the errors are DC.

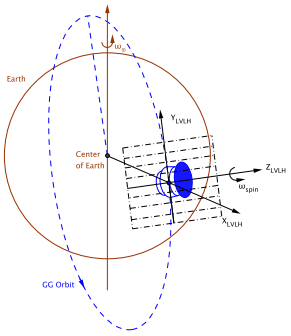

Figure 5: GG in its sun-synchronous orbit around the Earth and the Local vertical Local Horizontal reference frame.

If the phase angle of the output data is instead measured from a direction fixed in space (in this case we have a different time series $\varphi^{\star}_i$) the spin frequency is measured w.r.t the fixed stars (we call it $\nu^{\star}_{spin}$) and the same violation signal is at frequency $\nu^{\star}_{spin} \pm \nu_{orb}$. The inertial reference frame is centered at the center of mass of the Earth with GG orbiting as described before at frequency ν_{orb}; therefore it is $\nu^{\oplus}_{spin} = \nu^{\star}_{spin} - \nu_{orb}$ (if GG spins in the same sense as it orbits around the Earth). In case of violation the FFT of the output data will show a peak at $\nu^{\star}_{spin}$ ($\nu_{orb} = 1.7 \cdot 10^{-4}$ Hz while GG spins at 1 Hz, hence the modulation frequencies in the two cases are very close to each other). By demodulating to the non rotating frame (using the phase time series $\varphi^{\star}_i$) both signal and random errors are now at the orbital frequency.

We can see that in both cases we are upconverting the signal to the (high) spin frequency ($\nu^{\oplus}_{spin} \simeq \nu^{\star}_{spin}$) and the challenge is to reduce systematic errors at the orbital frequency. One such dangerous effect which is known to affect 1D sensors but is almost negligible in GG is the radiometer effect [28] [29].

2.4 Error budget, scientific requirements, traceability matrix and criteria for mission success

Table 1: GG error budget to $\eta = 10^{-17}$

Acceleration in X,Y Sensitive Plane Due to:	**Value of Acceleration (ms^{-2})**	**Frequency in Inertial Frame**	**Phase**	**Notes**
EP violation signal 10^{-17}	$8 \cdot 10^{-17}$	ν_{orb}	To Earth's center of mass (radial)	Frequency, phase and dependence on angle between spin axis and orbit normal perfectly known. TMs coupled with 540s period → **0.6 pm displacement to be detected**
Residual non-grav. perturbations (air drag, solar rad pressure, Earth's albedo, infrared rad)	$4 \cdot 10^{-17}$	ν_{orb}	Mostly along orbit (90° from signal)	Residual (from $2 \cdot 10^{-7}$ ms^{-2}) after DFACS & CMR
Earth's coupling to quadruple moments of TMs	$< 10^{-17}$	ν_{orb} & $3\nu_{orb}$	To Earth's center of mass (radial)	Effect at $3\nu_{orb}$ due to dependence on angle between spin axis and orbit normal (orbit precession discriminates from signal)
Tide coupled to radiometer along Z	$1.3 \cdot 10^{-15}$		To Earth's center of mass (radial)	Changes sign after half orbital period & Orbit precession discriminates further from signal (specific signature)
Tide coupled to thermal emission along Z	$3.8 \cdot 10^{-17}$			
Tide coupled to non grav accelerations along Z	$3 \cdot 10^{-17}$			
Tide due to whirl	$6.9 \cdot 10^{-14}$	ν_w, $\nu_w \pm \nu_{orb}$	To Earth's center of mass (radial)	Large frequency separation & Orbit precession discriminates further from signal (specific signature)
Tide due to center of mass offset	$2.4 \cdot 10^{-16}$	$2\ \nu_{spin}$	To Earth's center of mass (radial)	"High tide" twice per spin period: no issue
Magnetic moment of one TM coupled to $B_\oplus$ -induced magnetization of other	$8 \cdot 10^{-18}$	$2\nu_{orb}$	To Earth's center of mass (radial)	This is the largest magnetic effect. Reduced by μmetal shield of PGB by 10^{-2}, care with ferromagnetic impurities and magnetic susceptibility
Magnetic moments of TMs coupled to $B_\oplus$	$3 \cdot 10^{-20}$			
Coupling of $B_\oplus$-induced magnetic moments of TMs with each other	$4 \cdot 10^{-21}$	$4\nu_{orb}$		
Coupling of $B_\oplus$-induced magnetic moments of TMs with $B_\oplus$	$2 \cdot 10^{-22}$			
Direct radiometer effect in sensitive plane	Due to temperature differences in residual gas exposed to Earth infrared radiation. Competes directly with signal			Known to kill EP experiments, it is no issue even at room temperature due to spin
Free fall EP test with spinning TMs	Free fall acceleration of test masses may be affected by it spinning			Demonstrated not to be the case by enlarge
Electric charging of TMs	Inevitable because of cosmic rays, would impair the experiment			No issue due to passive electric grounding via mechanical suspensions. Direct momentum transfer negligible due to heavy TMs
Patches of electric charges on TMs	Mostly DC but also low frequency (ν_{orb}) component			Measured in lab prototype (both at zero spin and in rotation); with laser gauge gap large enough to make it negligible, it can be measured directly in orbit for firm check of detected signal. No issue.
Plasma at orbit altitude	Gives non gravitational acceleration in addition to neutral drag			Acceleration a few orders of magnitude smaller than neutral drag demonstrated. Plasma not allowed inside s/c by neutral+charged grid (tested with BeppoSAX). No issue
Eddy currents	Eddy currents losses in hollow conducting cylinders rotating in Earth magnetic field with component perpendicular to axis slow down the spin			Not relevant
Charging due to TMs rotation in Earth magnetic field	Occurs due to hollow conducting cylinders rotating in Earth magnetic field with component along axis			Not relevant
Thermal stability	Required mainly for thermal stability of TMs coupling arms (which provide Common Mode Rejection)			Required stability met. Spin makes most thermal changes unimportant. Uniform expansion of TMs not an issue; non uniform DC. SSO orbit with no eclipses helps.
Thermal noise at room temperature	Has an effect at signal (orbital) frequency			Computed for TMs coupled and spinning. With Q=20000 (measured) SNR=2 is obtained in half an hour. In 20 orbits (33 hr) we have a firm EP detection to 10^{-17}. Over 76 d assessment of detection (signal or disturbance?) made beyond question by dependence on inclination. 3 runs of 76 d each available in 9 months mission duration
Local mass anomalies	Affect test masses, couple to their quadrupole mass moments, DC as long as don't move (whole system co-rotating)			No read out saturation. No mass "sloshing" which would give effect at signal frequency. No issue
Spin axis	External torques may tilt the spin axis and affect measurement			s/c isolated in space + very high spin energy make spin axis essentially fixed in space
Satellite spin axis nutation	Spin-axis stabilized satellites undergo axis nutation which needs damping			Satellite outer shell weakly coupled to PGB (low Q=90 suspensions) provides damping
Spin rate	Variation of spin rate may affect measurement (through demodulation to non rotating frame)			Variations too small over measurement time. Co-rotation checked and maintained by DFC. Specific value of spin rate not relevant. Spin rate measured to 10^{-4} by spin rate optical sensor (breadboard available)
Active DFC Noise	Drag Free Control is always on (closed loop), thrusters fire at (close to) spin frequency			Major noise source at spin frequency and higher harmonics is also attenuated by PGB suspensions. No issue
Active whirl control noise	Capacitance actuators act on individual TMs (90° from radial at whirl frequency, far away from signal frequency)			Whirl control always OFF during science measurement, open loop, zero effect

Table 2: GG scientific requirements I

Driver #1: The Signal	
$\eta = 10^{-17}$	GG scientific objective
$sun-synchronous$	no eclipses
$h = 630km (a = 7008km)$	s/c orbit altitude, drag ≈ solar radiation pressure
$e \simeq 0.0$	eccentricity, almost circular orbit
$i \simeq 98^\circ$	sun-synchronous orbit inclination
$P_{orb} = 5.8 \cdot 10^3 s$, $\nu_{orb} = 1/P_{orb} = 1.713 \cdot 10^{-4} Hz$	GG orbit period and frequency
$g(h) = 8.12 m/s^2$	s/c local gravitational acceleration
$a_{EP} = g(h)\eta = 8.12 \cdot 10^{-17} m/s^2$	EP signal acceleration
$P_{DM} = 540s$	natural period of proof masses differential oscillation: $P_{DM} = \frac{2\pi}{\omega_{DM}}$
$\Delta x_{EP} = a_{EP} \cdot P_{DM}^2/(4\pi^2) = 0.6 \cdot 10^{-12} m$	proof masses displacement due to EP signal
$SNR = 2$	Signal to Noise Ratio (including systematic and random)
$T_{int} = 86400s - oneday-$	time duration of one experiment
Driver #2: External non gravitational forces	
$(A/M)_{GG} \leq 0.05 m^2/kg$	GG satellite maximum area to mass ratio
$a_{NGxy}(h) \leq 2 \cdot 10^{-7} m/s^2$	max. external non grav. acceleration in the sensitivity plane at the orbit altitude h
$\chi_{DFCxy} \leq 1/50000$	Drag Free Control rejection in the sensitivity plane
$\chi_{CMRxy} \leq 1/100000$	mechanical suspension Common Mode Rejection in the sensitivity plane
$\chi_{xy} = \chi_{DFCxy} \cdot \chi_{CMRxy} \leq 2 \cdot 10^{-10}$	maximum total rejection in the sensitivity plane
$a_{CMxy} = a_{NGxy} \cdot \chi_{DFCxy} \leq 4 \cdot 10^{-12} m/s^2$	max. common mode non grav. acc. (on PGB and TMs) in the sensitivity plane
$P_{PGB} = 360s$	PGB natural oscillation period in the sensitivity plane
$\Delta r_{PGB} = a_{CMxy} \cdot P_{PGB}^2/(4\pi^2) = 1.3 \cdot 10^{-8} m$	maximum PGB displacement due to residual uncompensated external non grav. acceleration in the sensitivity plane
$P_{CM} = 30s$	test mass Common Mode oscillation period in the sensitivity plane
$\Delta r_{CMxy} = a_{CMxy} \cdot P_{CM}^2/(4\pi^2) \leq 9.1 \cdot 10^{-11} m$	maximum test mass common mode displacement in the sensitivity plane
$a_{DMxy} = a_{NGxy} \cdot \chi_{DFCxy} \cdot \chi_{CMRxy} \leq 4 \cdot 10^{-17} m/s^2$	maximum differential mode non grav. acceleration on test masses in the sensitivity plane
$a_{NGz}(h) \leq 5 \cdot 10^{-8} m/s^2$	maximum external non grav. acceleration along the spin axis at the orbit altitude h
$\chi_{DFCz} \leq 1/500$	Drag Free Control rejection along the spin axis
$\chi_{CMRz} \leq 1/50$	mechanical suspension Common Mode Rejection along the spin axis
$\chi_z = \chi_{DFCz} \cdot \chi_{CMRz} \leq 4 \cdot 10^{-5}$	maximum total rejection along the spin axis
$a_{CMz} = a_{NGz} \cdot \chi_{DFCz} \leq 10^{-10} m/s^2$	maximum common mode non grav. acceleration (on PGB and test masses) along spin axis
$P_{PGBz} = 30s$	PGB natural oscillation period along spin axis
$\Delta z_{PGB} = a_{CMz} \cdot P_{PGBz}^2/(4\pi^2) = 2.28 \cdot 10^{-9} m$	maximum PGB displacement due to residual uncompensated external non grav. acceleration along spin axis
$P_z = 30s$	test mass Common Mode oscillation period along spin axis
$\Delta z_{CM} = a_{CMz} \cdot P_z^2/(4\pi^2) \leq 2.28 \cdot 10^{-9} m$	maximum test mass common mode displacement along spin axis
$a_{DMz} = a_{NGz} \cdot \chi_{DFCz} \cdot \chi_{CMRz} \leq 2 \cdot 10^{-12} m/s^2$	maximum differential mode non grav. acceleration on test masses along spin axis
$\chi_{bridge} = \Delta x_{EP}/\Delta r_{CMxy} \simeq 6.6 \cdot 10^{-3}$ $d_{bridge} = 5mm \quad \Delta d_{bridge} \simeq 33\mu m$	max. cap bridge mechanical unbalance d is the bridge gap and Δd is the bridge unbalance
Driver #3: Test bodies mass moments	
$\lvert\Delta J/J_x\rvert_{TMs} \leq 1.2 \cdot 10^{-2}$	test masses maximum fractional difference between principal moments of inertia. $\Delta J = J_z - J_x$
$a_{QP}^{\oplus} \leq 0.5 \cdot a_{EP}$	maximum differential acceleration due to Earth monopole coupling with TMs quadrupole moments (same frequency and phase of EP signal)
$\Delta x_{QP}^{\oplus} \leq 0.5 \Delta x_{EP}$	max. differential displacement due to Earth monopole coupling with TMs quadrupole
Driver #4: Whirl Motion	
$Q_{PGB}(\omega_{spin}) = 90$	mechanical quality factor of the PGB-s/c suspension (at the spin frequency)
$(r_w)_{PGB} \leq 10^{-8} m$	maximum PGB whirl displacement (closed loop)
$Q_{TMs}(\omega_{spin}) \geq 20000$	mechanical quality factor of the TMs suspension (at the spin frequency)
$(r_w)_{TMs} \leq 10^{-8} m$	maximum TMs whirl displacement (closed loop)
$k_{safety} = 1.5$	safety gain of TMs whirl control
$\delta\varphi \leq 0.14^\circ$	maximum TMs whirl control phase error
Driver #5: Satellite spin frequency	
$P_{spin} = 1s, \nu_{spin} = 1/P_{spin} = 1Hz$	ν_{spin} s/c spin frequency w.r.t. LVLH Reference Frame, $\omega_{spin} = 2\pi\nu_{spin}$
$\nu_{spin}^* = \nu_{spin} + \nu_{orb} = 1.0001713Hz$	s/c spin frequency w.r.t. IRF
$(\Delta\nu_{spin}/\nu_{spin}) \leq 10^{-5} \div 10^{-4}$	maximum fractional error of the knowledge of the s/c spin frequency
Driver #6: Earth Tides	
$(\varepsilon_{mech})_{PGB} \leq 10^{-4} m$	maximum mechanical mounting error –offset- for the PGB
$(\varepsilon_{mech})_{TMs} \leq 10^{-5} m$	maximum mechanical mounting error –offset- for the TMs
G_{ij} $[m/s^2/m]$	gravity gradient tensor: $G_{xx} \approx 3.5 \cdot 10^{-6}$ 1/s, $G_{xz} \approx 1.6 \cdot 10^{-6}$ 1/s
$a_{ETwhirl} = 2 \cdot G_{xx} \cdot (r_w)_{TMs} \approx 7 \cdot 10^{-14} m/s^2$	maximum tidal signal in the sensitivity plane due to coupling of gravity gradient with whirl radius: frequency is very far from EP signal one
$\Delta z_{DM} = a_{DMz} \cdot P_z^2/(4\pi^2) \approx 4.6 \cdot 10^{-11} m$	maximum TM differential displacement along spin axis due to residual non gravitational force acting along the s/c symmetry axis
$a_{ET\_NGz} = G_{xz} \cdot \Delta z_{DM} \approx 7.3 \cdot 10^{-17} m/s^2$	maximum tidal signal in the sensitivity plane due to coupling of gravity gradient with TMs differential displacement along spin axis generated by residual drag along s/c symmetry axis: frequency is $2^*\nu_{orb}$
$\Delta z_{radiom} = \frac{^p{}_{PGB} \cdot \lvert\frac{1}{\rho_1} - \frac{1}{\rho_2}\rvert}{2 \cdot m \cdot T \cdot \frac{\Delta T}{\Delta z}} \cdot \frac{P_z^2}{4\cdot\pi^2} \approx 2.0 \cdot 10^{-9} m$	maximum differential displacement along spin axis due to radiometric effect along z; m mass, ρ_i masses density, T temperature, $\Delta T/\Delta z$ thermal gradient along spin axis.
$a_{ET\_radiom} = G_x z \cdot \Delta z_{radiom} \approx 3 \cdot 10^{-15} m/s^2$	maximum tidal signal in the sensitivity plane due to coupling of gravity gradient with TMs differential displacement along spin axis generated by radiometric effect: frequency is $2^*\nu_{orb}$
$\Delta z_{em-rad} = \frac{4\sigma_{SB} T^3 \cdot \lvert(S_1\varepsilon_1\Delta T_{z1} - S_2\varepsilon_2\Delta T_{z2})\rvert}{m \cdot c} \cdot \frac{P_z^2}{4\cdot\pi^2} \approx 5.3 \cdot 10^{-11} m$	maximum differential displacement along spin axis due to test masses emitted radiation (top and bottom surfaces different temperature). σ_{SB} Stefan-Boltzmann constant, ε_i test masses emissivity, c speed of light.
$a_{ET\_em-rad} = G_{xz} \cdot \Delta z_{em-rad} \approx 8.4 \cdot 10^{-17} m/s^2$	maximum tidal signal in the sensitivity plane due to coupling of gravity gradient with TMs differential displacement along spin axis generated by test masses emitted radiation: frequency is $2^*\nu_{orb}$
Driver #7: Temperature	
$N_{days} \geq 20d$	minimum number of days between two consecutive test masses rebalancing
$\dot{T} \leq 0.2K/d$	maximum test masses daily temperature variation
$\Delta T/\Delta z \leq 4K/m$	maximum temperature gradient along axis
$(\alpha_{CTE})_{TMs} \leq 2 \cdot 10^{-5} K^{-1}$	maximum thermal expansion coefficient of test masses
$(\alpha_{CTE})_{ca} \leq 10^{-5} K^{-1}$	maximum thermal expansion coefficient of coupling arms
$\Delta k/k \leq 4 \cdot 10^{-4} K^{-1}$	maximum fractional thermal variation of suspension stiffness
$\chi_k \leq 1/100$	maximum relative change in stiffness of suspension with temperature
$p_{PGB} \leq 10^{-7} torr \quad (p_{PGB} \leq 1.333 \cdot 10^{-5} pascal)$	maximum residual pressure inside the PGB
$\epsilon_{gold-coating} \leq 3 \cdot 10^{-2}$	gold coating emissivity
$\hat{x}(\omega) = \frac{1}{\omega_{DM}^2} \cdot \sqrt{\frac{4 \cdot K_B T \cdot \omega_{DM}}{mQ\omega_{spin}(\omega_{spin}/\omega_{DM})}} = 9.1 \cdot 10^{-12} m/\sqrt{Hz}$	Spectral Density of thermal noise displacement; K_B Boltzmann's constant

Table 3: GG scientific requirements II

Driver #8: Magnetic Coupling	
$\chi_{\mu shield\_PGB} \leq 1/100$	minimum magnetic field reduction provided by mu-metal shielding of PGB
$(\chi_m)_{TMs} \leq 10^{-6}$	maximum test masses magnetic susceptibility
$\mu_{TMs} \leq 10^{-6} Am^2$	maximum test masses inner magnetic moment
$a_{\chi_1\mu_2} \approx \frac{\chi_1 V_1 B_{orbit} \chi_{\mu shield\_PGB}}{m \cdot r^4} \mu_2 \leq 8 \cdot 10^{-18} m/s^2$	maximum differential acceleration due to coupling of one test mass with magnetic moment and the other with Earth B field induced magnetization: frequency is $2^*\nu_{orb}$. V_i mass volume, r test mass dimensions.
$a_{\mu_2 B_\oplus} \approx 3 \cdot \mu_2 \cdot \frac{B_{orbit} \chi_{\mu shield\_PGB}}{m \cdot (R_\oplus + h)} \leq 3 \cdot 10^{-20} m/s^2$	maximum differential acceleration due to coupling of one test mass inner magnetic moment μ with Earth B field: frequency is $2^*\nu_{orb}$. $R_\oplus$ Earth radius.
$a_{\mu_1\mu_2} \approx \frac{\mu_{vac} \cdot \mu_1 \cdot \mu_1}{m \cdot r^4} \leq 1.4 \cdot 10^{-15} m/s^2$	maximum differential acceleration due to coupling of test masses inner magnetic moment: acceleration is DC in s/c. μ_{vac} vacuum permeability.
$a_{\chi_1\chi_2} \approx \frac{\chi_1 V_1 \cdot \chi_2 V_2 \cdot \chi^2_{\mu shield\_PGB} B^2_{orbit}}{\mu_{vac} \cdot m \cdot r^4} \leq 4 \cdot 10^{-21} m/s^2$	maximum differential acceleration due to coupling of test masses through their Earth B field induced magnetization: frequency is $4^*\nu_{orb}$
$a_{\chi_1 B_\oplus} \approx 3 \cdot \frac{\chi_1 V_1 \cdot \chi^2_{\mu shield\_PGB} B^2_{orbit}}{\mu_{vac} \cdot m \cdot (R_\oplus + h)} \leq 2 \cdot 10^{-22} m/s^2$	maximum differential acceleration due to coupling of one test mass with induced magnetization with the Earth B field: frequency is $4^*\nu_{orb}$
$a_{\chi_1 B_\oplus} \approx 3 \cdot \frac{\chi_1 V_1 \cdot \chi^2_{\mu shield\_PGB} B^2_{orbit}}{\mu_{vac} \cdot m \cdot (R_\oplus + h)} \leq 2 \cdot 10^{-22} m/s^2$	maximum differential acceleration due to coupling of one diamagnetic test mass with induced magnetization with the Earth B field
Driver #9: Electric Charging	
no charging	mechanical connections prevent test mass charging
patch effects no issue	measured in GGG, can be measured in space, large gaps, even larger with laser gauge

Science goal	First detection of physical fields beyond the Standard Model of particle physics, by discovery of violation of the Equivalence Principle	
Science objective	Detection of differential acceleration between test masses of different materials falling in the gravitational field of the Earth to fractional accuracy $\Delta a/a < 1 \cdot 10^{-17}$	
Scientific measurement requirements	**Instrument performance requirements**	**Mission requirements (top level)**
$\Delta a/a < 1 \cdot 10^{-17}$		- Near-circular 600km SSO - 1 Hz spin - Spin axis close to orbit normal - Spin axis reorientation manoeuvres
Relative displacement of the rotation axes of 2 coaxial test masses in the plane perpendicular to the common rotation axis $\Delta rXY < 0.5pm\ (rms)$	- Cap sensor resolution: < 0.1 pm - Differential period of TM suspensions in XY plane > 540s - Instrument $CMRR(XY) < 1 \cdot 10^{-5}$ - Integration time >1800 s -	Non gravitational acceleration limit $a_{NG,XY} < 2 \cdot 10^{-7} m/s^2$ - DFC rejection in XY plane $< 2 \cdot 10^{-5}$ in MBW
Relative displacement of the centres of 2 coaxial test masses along the Z axis $\Delta z < 500pm$	- Cap sensor resolution: $< 100pm$ - Common mode period of TM suspensions (Z-axis) > 30s - Instrument CMRR(Z) $< 2 \cdot 10^{-2}$ - Fine regulation by inch worms (PZT) < 100 pm	- DFC rejection along Z $< 2.5 \cdot 10^{-3}$ - Temperature drifts, temperature time gradients, temperature gradients across the balance arms - Calibration by nulling of tidal signal
Relative displacement of the rotation axis of the lab (PGB) w.r.t. the common TM rotation axis, in the XY plane $\Delta rXY < 10\ nm\ (rms)$	- Cap sensor resolution: < 1 nm rms - Common mode period of the TM suspensions in the XY plane 30s < T <100s - Q(TM) > 20000	- Whirl control once in 100 orbits - TM temperature < 300°K - Residual pressure acting on the test masses $< 1 \cdot 10^{-5} Torr$
Relative displacement of the centres of PGB and TMs, along the Z axis $\Delta z < 0.5pm$	- Cap sensor resolution < 0.1 pm (*) - Common mode period of the TM suspensions in the Z direction = 30s	
Relative displacement of the rotation axis of the S/C and PGB, in the XY plane $\Delta rXY < 30nm$	- Cap sensor resolution < 3 nm (*) - Natural frequency of the PGB suspension in XY plane = 1/360s - Q(PGB) > 90	
Relative displacement of the centres of S/C and PGB, along Z axis $\Delta z < 300nm$	- Cap sensor resolution < 30 nm (*) - Natural frequency of the PGB suspension in Z direction = 1/30s - Q(PGB) > 90	
Phase lag between S/C and PGB around Z axis $\Delta\phi < 5 \cdot 10^{-5} rad$	- Cap sensor resolution $< 1 \cdot 10^{-6} rad$	- Attitude rate control loop - Spin rate control loop
Spin rate stability $\Delta\omega/\omega < 1 \cdot 10^{-4}$	- Spin rate sensor resolution $< 1 \cdot 10^{-6} \omega$	- Spin axis vector knowledge < 1°
(*) Max displacement of TM w.r.t. PGB << 0.15 mm		

Table 4: Science requirements traceability matrix. The table shows how the main measurement requirements map into requirements of the experiment apparatus and of the mission design. The differential acceleration goal leads to requirements on the orbit (altitude, eccentricity) and attitude (spin rate and orientation). The basic measurements are picometer-level displacements, in-plane and out-of-plane, leading to requirements on the natural frequency of the suspensions, the resolution of the position sensors, and the common-mode rejection ratios. These, in turn, dictate the needs in terms of drag control and whirl control.

Science Requirements	$\eta = \Delta a/a$	**Top-level experiment requirement**
Nominal	10^{-17}	Sum of all known sources of systematic error $< 8 \cdot 10^{-17}\mathrm{m/s^2}$
Minimum	10^{-16}	Unexpected performance degradations leading to systematics $< 8 \cdot 10^{-16}\mathrm{m/s^2}$
Goal	10^{-18}	Sum of all sources of systematic error after the fact $< 8 \cdot 10^{-18}\mathrm{m/s^2}$

Table 5: Criteria for mission success. GG will make a full measurement to 10^{-17} in 1 d. The nominal mission encompasses 9 months with 230 days dedicated to science measurements. Therefore the mission has the potential of reaching 10^{-18}, provided that systematic errors are reduced accordingly. The nominal science requirement is defined as 10^{-17}, based on the current error budget (see Table 1). The minimum science requirement is defined as 10^{-16}, caused by so far unidentified performance degradations which might arise during the implementation phase. The advanced goal is defined as 10^{-18} and it may be reached if the mission lasts as long as planned and the systematic errors turn out to be lower than we estimate today using worst case models.

3 GG mission profile

In the past, versions of GG have been studied for ASI in both near-equatorial orbit and sun-synchronous orbit (SSO). The near equatorial orbit has the advantage that the orientation of the spin axis naturally remains close to the normal to the orbit plane. On the minus side, the orbit passes in the Earth's shadow once per orbit, leading to temperature perturbations that may interfere with the experiment. The SSO is eclipse-free for most of the year but the spin axis necessitates periodic manoeuvres to keep it close to the orbit normal, where the signal is maximum. In SSO, we can turn the precession of the orbit normal around the spin axis into an advantage by performing *null checks* (checks for systematic effects that depend on the angle between the spin axis and the orbit plane).

The orbit selected for GG is near-circular, sun-synchronous (SSO), dawn-dusk with the perigee around 600 km. The corresponding sun-synchronous inclination is $\simeq 98.4^{\mathrm{o}}$. SSO is a standard destination for Vega. According to the User's manual, the launcher can inject more than 1400 kg in this orbit. GG will use up 400 kg, i.e. less than 30% of the full payload capability.

The selected orbit has one eclipse season per year with maximum shadow time per orbit of about 21 minutes. The eclipse season can always be made to occur about 8 months after beginning of mission.

In SSO, without dedicated manoeuvres, the GG spin axis will always point to the same inertial direction, whereas the orbit plane will precess at about $1\,^{\mathrm{o}}$/d. The signal is in the orbit plane and, to maximise the chances of detecting it, there must be a significant period of time in which the spin axis of the satellite stays close to the normal vector to the orbit plane. Therefore, spin axis reorientation manoeuvres are needed. In the designed 9-month duration of the mission only 2 such manoeuvres are needed for the following reasons.

The amplitude of the angle between the spin axis and the orbit normal is limited by the illumination of the solar cells. Assuming that we limit the sun incidence on the top array to 45^{o}, 4 reorientation manoeuvres per year would be necessary. The magnitude of the target signal oscillates between 70% of maximum ($\cos 45^{\mathrm{o}}$) and maximum, providing significant modulation for *null checks* against systematic errors since the signature of the signal is known exactly. The time interval period between 2 successive spin axis manoeuvres is about 90 d. Therefore, over a design lifetime of 9 months, only two such manoeuvres need to be planned. Before each manoeuvre, the test masses are locked in place using the fine lockers (inch worms). The reorientation is executed by Nitrogen thrusters with small specific impulse, therefore several hours are required. After the manoeuvre, the test masses are released and the system is recalibrated.

No orbit change manoeuvres are required after acquisition of the operational orbit. Due to the very low thermal noise and short integration time allowed by the sensor [17], [21] a full measurement is performed in 1 d. Then, the experiment is conducted in measurement intervals lasting about 2 weeks. Initially, each measurement interval will be followed by a calibration session. As the mission progresses, one will learn whether such frequent recalibrations are needed. The data volume generated is about 2.4 Gbit/day. Such amount of data can be transmitted to one ground

station in four 10-minute passes per day at a telemetry rate of 1 Mbit/s. The processing of the scientific data is done in bulk; therefore no scientific quick-look is required. All scientific operations are autonomous, executed on the basis of time-tagged operation sequences that are loaded at least one day in advance. Given the high level of autonomy, the tasks of the ground control are essentially limited to:

- Commanding and monitoring of the attitude manoeuvres (spin axis reorientation); twice over 9-month mission lifetime
- Generation and transmission of command sequences and parameters
- Analysis of satellite data to establish that the satellite is operating correctly.

4 GG payload

The GG payload is constituted by the PGB (Pico Gravity Box) laboratory enclosing the test masses (see Fig. 6) with their read-out system and the control electronics (see Fig. 7). The mechanical layout of the PGB comprises:

– the two cylindrical Test Masses (TMs)

– small capacitance sensors/actuators for sensing relative displacements and damping the whirl motions

– suspension springs and coupling arms

– inch-worms and piezo-ceramics for fine mechanical balancing and calibration

– PGB outer shell, providing a controlled thermal enclosure, μmetal shielding and support to the capacitance bridge read out (or to the laser beam launchers in case of laser interferometry read-out; see below)

– launch-lock mechanisms, associated to all suspended bodies.

The PGB also carries 2 small mirrors, in correspondence of photo-detectors mounted on the inner surface of the spacecraft, for measuring small residual phase lags with respect to the spacecraft.

It is important to stress that the GG payload was designed from the start taking care that the required vacuum be obtained by venting to outer space, so as not to be in need to launch a vacuum chamber, which would be more costly. This requires not to let the surrounding plasma inside the s/c; the issue has been investigated and can be solved as tested in the BeppoSAX mission. Appropriate apertures to open space can also take care of outgassing.

Fig. 6 shows (to the right) the test cylinders assembled around the central shaft of the PGB with a detail of the capacitive plates (in yellow) of the read-out system. These plates are in all similar to those currently used on the GGG prototype, which are well visible in Fig. 8. The capacitance sensing noise relies on the GGG experience and heritage from the ISA-type accelerometer built at INAF-IAPS for the BepiColombo mission by V. Iafolla and his group. Fig. 6 also shows (to the left) a section along the spin/symmetry axis displays the PGB enclosure and shaft and the concentric test cylinders (in blue and green) inside it; in this case the laser metrology system is sketched, which would be implemented in case of JPL-NASA participation, with the laser beam launchers located on the PGB.

The payload electronics includes:

– the PGB Control and Processing Electronics (CPE), located on the spacecraft platform, managing PGB motion control (whirl sensing, whirl damping and drag-free control) and processing of all signals coming from the test masses (motion control and EP sensing)

– the Experiment Control Electronics (ECE), housed inside the PGB, and communicating with the CPE via an optical link. The ECE, under control of the CPE processor, locally manages whirl sensing and damper activation, and inch worm activation for fine adjustment of the test mass position along Z.

The payload apparatus further includes the necessary electrical harness and connectors and the thermal insulation and μmetal shielding.

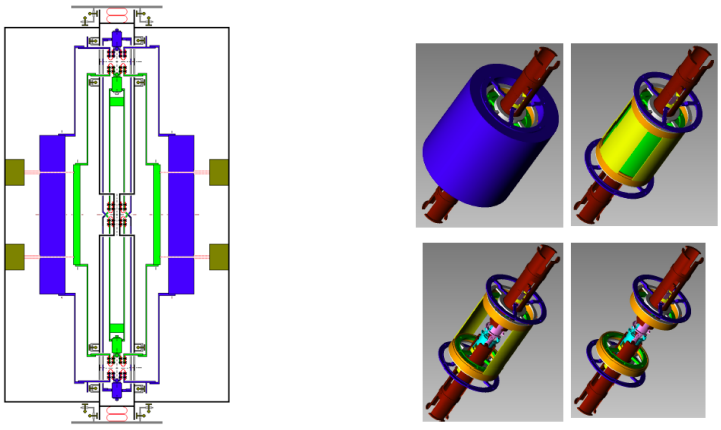

Figure 6: The GG sensor made of 2 coaxial concentric test cylinders (in green and blue) spinning around the symmetry axis and weakly coupled in the plane perpendicular to it. *Right*: components of the sensor from the outside in. The blue and green cylinders are the test masses; the yellow plates are the capacitance bridge plates located halfway in between the test cylinders to measure their relative displacements along the two orthogonal directions of the plane perpendicular to the symmetry axis. They are similar to the plates used in GGG (see Fig. 8) The brown central tube is the PGB shaft. *Left*: section along the spin axis of the GG sensor/balance as described in Fig. 1. In addition to the test cylinders at the center it shows the enclosing PGB with the springs which connect it to the spacecraft outer shell (not shown).

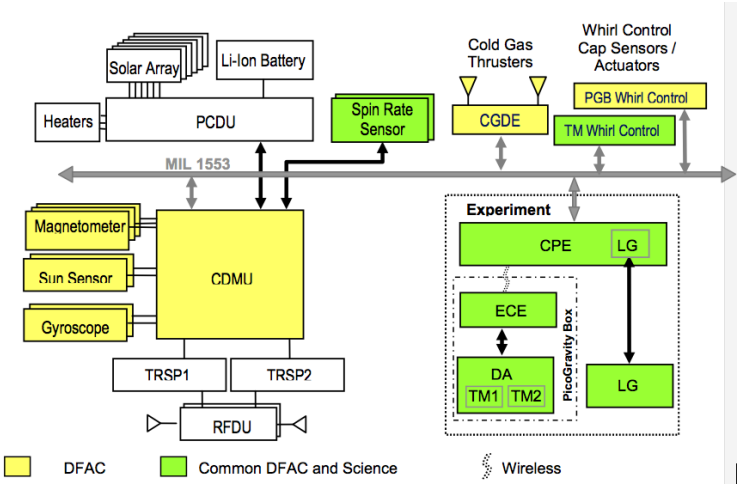

Figure 7: Instrument block diagram

In the event of a participation of JPL, the capacitance read-out will be replaced by a laser gauge. Laser metrology is linear and more sensitive than the cap sensors. Most importantly, it allows larger gaps between the test masses (2 cm or more are allowed) making gas damping irrelevant and electric charge patch effects negligible. In addition, it is purely differential (while cap sensors need to be centered in between the test cylinders). Last but not least, the equipment can be installed on the experiment with minimal mass and volume impact (see Fig. 6 left). Fig. 9 shows a schematic of the system. The Laser Metrology system comprises 6 laser beam launchers attached to the PGB shell, 6 laser beam targets, attached to the test masses, and control electronics, included as a module in the CPE. Small holes are drilled in the outer cylinders to let light get to the inner cylinder. The beam targets the lasers measure to are polished and coated parts of the test cylinders. The measurement is the difference of the average of the measurements of the X,Y displacements of the outer test mass and the inner test mass.

Launch locks are needed to protect from the launch loads the experiment elements that, in orbit, are suspended on weak U-shape flexure springs. Locking against large accelerations is only

Figure 8: The capacitance cage currently used for the read-out of the GGG prototype (2 cap bridges in 2 perpendicular directions). *Left*: the cage during manufacture showing 4 brass plates. *Right*: engineering drawings showing the cap cage rigidly mounted on the shaft and the assembled with the test cylinders and the coupling arm of the GGG prototype balance.

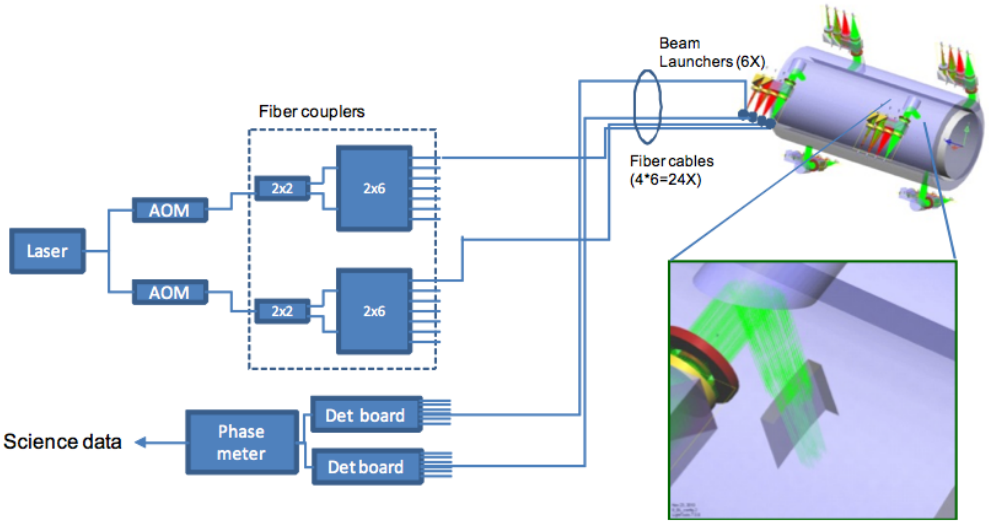

Figure 9: Schematic layout of the laser metrology system

required during the launch phase. During the mission, the spring-suspended elements need to be secured when spin-axis reorientation manoeuvres occur (3 times during the entire duration of the mission). The accelerations applied in such cases are much smaller than the launch loads, and locking/unlocking will be performed by means of appropriate inch-worms as shown in Fig. 10, right hand side.

The following elements are launch-locked, from the outside in: (1) the whole PGB (2) the outer test mass (3) the inner test mass (4) the balance arms connected to both test masses via thin cantilever springs. The GG launch lock design requirements are not demanding: the test masses are physically large; there is no requirement on position and velocity after releasing the lock (the flexures and supercritical rotation provide alignment); the mechanisms are operated only once. Thus, micro-positioning, space-saving packaging and fine-tuned release are not required, nor is mechanism repeatability.

A design and analysis exercise of the launch locks is available. To simplify and optimise the design, the same concept was employed on all four levels. The locking is based on two sets of identical non-magnetic actuators able to withstand the launch accelerations. The actuators can be procured off the shelf (Physics Instruments). The load components acting in directions perpendicular to the satellite symmetry axis are handled by custom made tips of the actuator plungers matching corresponding indents of the counterpart to be locked (figure). Finite element analysis of the mechanisms was performed. All locks were found very stiff, meaning that the mechanical configuration selected is adequate and no further locking areas need to be considered in the detailed design phase.

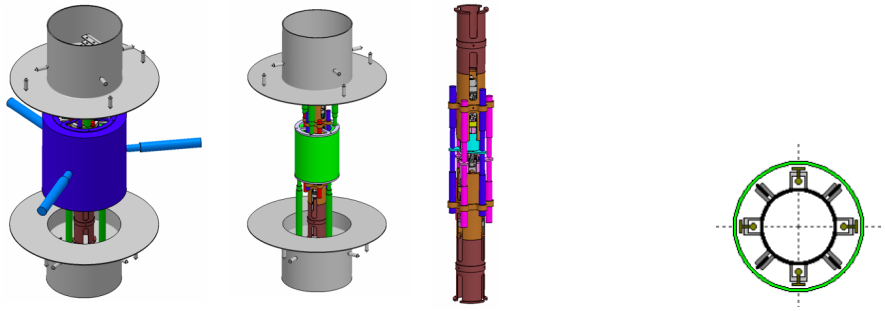

Figure 10: *From left to right:* hard launch lock mechanisms of the outer (blue) test cylinder locking it to the PGB body; of the inner (green) test cylinder locking it to the PGB body; of the PGB central shaft (brown) locking it to the s/c shell. In this way there is no relative motion affecting the U-shaped flexures. Once unlocked after launch they will not need to be used again. For comparison, the height of the outer test cylinder is 29 cm. *Further right*: one of the fine lock-unlock system based on inch-worms (section perpendicular to the spin/symmetry axis) to be used during space attitude manoeuvers for 3 times during mission. There are 4 inch-worms at 90° from each other which can adjust the motion of each mass w.r.t. the PGB shaft. The diameter of the inner circle is that of the PGB shaft. In between the inch-worms (at 45°) are 4 small capacitance sensors/actuators for damping of even slower whirl motions.

A key component of the GG payload are very weak (in absence of weight) U-shape flexures (as sketched in Fig. 6) which allow very weak coupling of the test cylinders while also providing electric grounding. Springs, and high quality springs in particular, are very old tools whose theoretical elastic properties are very well established. Manufacturing, simulation and testing techniques are also well established. Fig. 11 shows how the elastic properties of U-shape flexures are measured in the lab with a simple set-up (left), and how the losses of a helical spring, unaffected by local gravity, is measured (right) to demonstrate that the level of losses (Q=20000) required in GG can be obtained and experimentally verified.

Losses have also been measured for the mechanical suspensions of the GGG prototype with the system fully assembled, as shown in Fig. 12. We can say that mechanical suspensions are well known and very reliable tools which absence of weight allows us to push to their limiting weakness, thus making them sensitive to extremely small forces.

Finally, we have developed ways of suspending and putting in oscillation the test cylinders (10 kg each) in order to measure (and adjust if needed) their moments of inertia so as to verify experimentally that the requirements on quadrupole mass moments are met. These methods of old classical mechanics are also well established.

The total mass budget of the GG payload is reported in Table 6. For the power budget see Table 9.

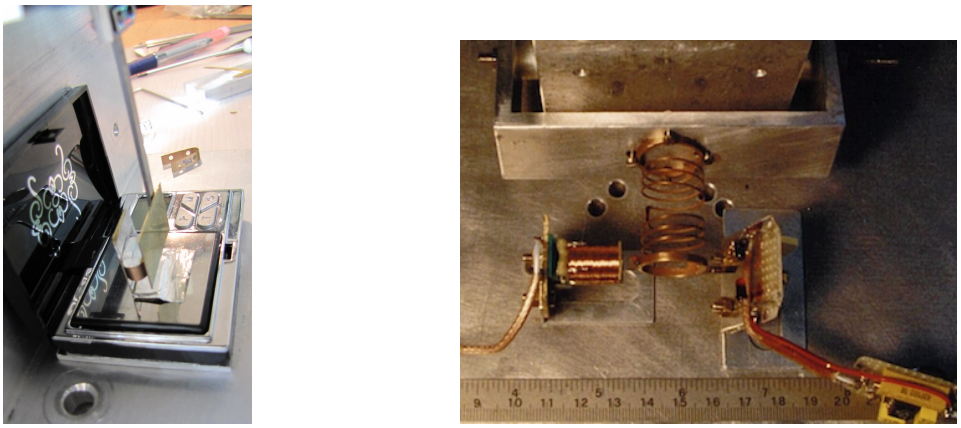

Figure 11: *Left:* A simple set-up is used to measure all the relevant elastic constants of U-shape flexures like those to be used in space to couple the GG test cylinders. The measurements allow us to firmly establish that the required natural frequencies are obtained. *Right*: A helical spring was manufactured in CuBe by electroerosion from a single block to measure its losses in horizontal at frequencies of 1 to a few Hz. The measured Q was close to 20000, demonstrating that the GG requirement can be met even with a rather complicated spring shape. CuBe is an alloy well known for its high mechanical quality, whose manufacturing and thermal treatment procedures are well established.

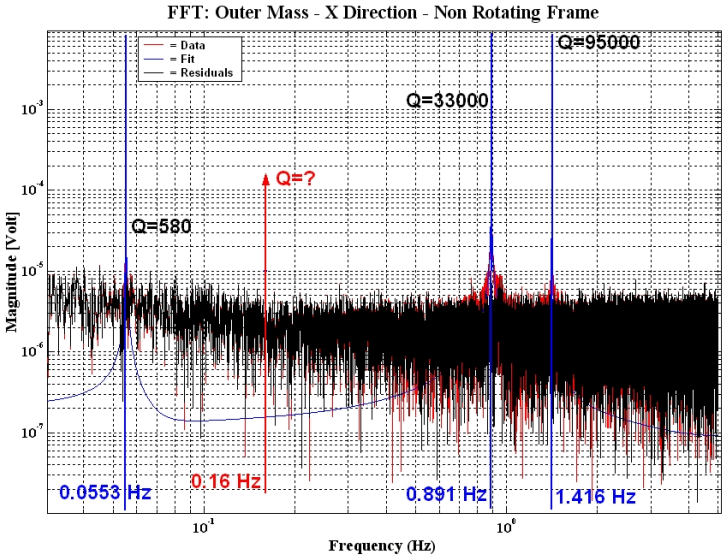

Figure 12: Resulting quality factors of the GGG prototype at the natural frequencies (at zero spin) as obtained by measuring the oscillation decay of the full assembled system. The blue curve is the FFT of the fitted output data. (Fig. 5 of [30]). The plot shows that at the 1 Hz spin frequency of GG, at which the relevant losses occur, the required quality factor Q=20000 can be achieved.

Table 6: Payload mass budget

Item	No.	Unit Mass [kg]	Total Mass [kg]	Margin[%]	Total mass with margin [kg]
Inner Test Mass	1	10.0	10.0	0	10.0
Outer Test Mass	1	10.0	10.0	0	10.0
PGB Shaft			2.9	20	3.5
PGB Shell	1	12.25	12.3	20	14.7
μmetal on PGB shell	1	1.76	1.8	20	2.1
PGB interface spring	8	0.11	0.9	20	1.0
Plasma grid allocation	4	0.01	0.0	20	0.0
Locking mechanisms	4	2.00	8.0	20	9.6
Inch Worms	14	0.10	1.4	20	1.7
Experiment Control Electronics	1	4.50	4.5	20	5.4
Control & Processing Electronics	1	6.00	6.0	20	7.2
Payload Total			**57.7**	**13.1**	**65.2**

5 System requirements and spacecraft key issues

Table 7 summarises the flow-down from experiment/mission requirements to the space and ground segment system requirements. The required orbit is near circular, near polar (sun synchronous). The putative EP violation signal has magnitude proportional to $1/r^2$ and is directed at the centre of the Earth. Therefore the orbit should be as low as possible; the design perigee altitude, 600 km, is chosen to limit the magnitude of the disturbing air drag acceleration. A small eccentricity will help distinguish the violation signal from disturbing accelerations such as those due to multipoles of the Earth's gravity. The mass is compatible with the VEGA launcher in a piggy-back configuration (Table 9).

An essential feature of the GG experiment is its fast spin of 1 Hz. All parts of the apparatus and the satellite co-rotate around a common symmetry axis. By spinning the satellite and the accelerometer, with its displacement transducer, around their common symmetry axis, the EP violation displacement signal is modulated at the spin frequency of the system relative to the centre of the Earth. Spin speed is chosen to optimize the stability of the experiment and satellite. Due to the very weak coupling between the masses and rapid spin, the GG system is a rotor in supercritical regime, self-centring within the fabrication and mounting errors. Moreover, the spacecraft too is passively stabilized by rotation around its symmetry axis. Nutation damping is provided by a passive device (the Pico Gravity Box, PGB) and no active attitude control is required for the duration of each data-collection period. Both the spin and the experiment impose mild requirements on the mass distribution on board and the inertia ratios.

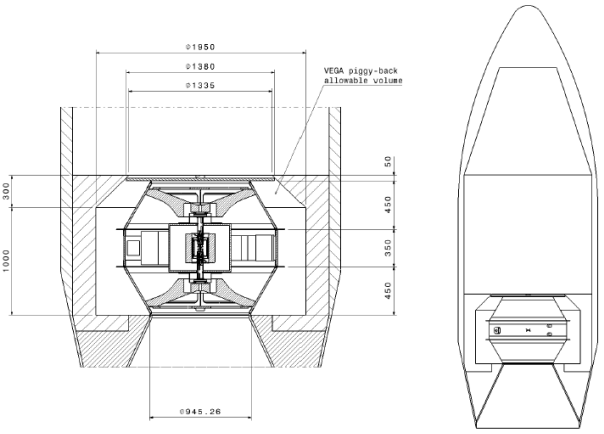

Figure 13: GG spacecraft accomodated inside VESPA piggy back adapter of the VEGA launcher

The EP violation signal is sought in a narrow frequency band around the orbit frequency. Effects occurring in this band, such as air drag components and temperature variations driven by the satellite's revolution around the Earth, will directly compete with the signal. Air drag has components at the orbit frequency (e.g. the diurnal bulge), although displaced in phase from the signal by 90°, and it must be counteracted actively by drag free control. Temperature variations driven by the orbital eclipse will be absent for most of the year thanks to the SSO. The satellite design in concentric shells makes it heavily insulated and analysis shows that the temperature variations of the external environment are not communicated to the test masses.

The satellite's configuration requirements include: compatibility with launcher vehicle fairing envelope; cylindrical symmetry; easy integration of payload module (PGB); low area-to-mass ratio; the spin axis must be a principal axis of inertia; the spin axis moment of inertia must be greater than the transverse moment of inertia. These requirements do not allow reuse of a standard platform. The proposed solution is an ad-hoc structure with high cylindrical symmetry, supporting the PGB and equipment. The spacecraft body is about 1.5 m wide and 1.2 m high (Fig. 13). The experimental apparatus is accommodated in a nested arrangement inside the body. The spacecraft structure, similar to a spinning top, is exceptionally compact and stiff. It is made up of a central cylinder and an upper and lower truncated cone. The central belt is used for mounting equipment, including thrusters and sensors; this solution also allows a suitable distribution of thermal covers and radiators to realize an efficient thermal control. The upper cone is removable to allow the integration of the PGB with its suspension springs; the lower cone supports the launcher interface ring. Sensors and electric thrusters are mounted to the central belt. Two S-band patch antennas provide spherical coverage. The solar array is mounted on top on a circular substrate.

Table 7: Flow-down mission requirements

Mission Requirements	Mission Design Requirements	Spacecraft Requirements	Ground System Requirements	Operations Requirements
Signal Strength	Low Earth Orbit, near-circular	Spin axis near-perpendicular to orbit plane		Spin axis reorientation every 3 months, to realign spin axis to orbit normal after orbit plane precession
Signal identification	Mission length: 9 months	Spin stabilized s/c 1 Hz spin rate. Fractional difference of inertia moments $0.2 < \Delta I/I < 0.3$		Ephemeris accuracy: knowledge of direction to Earth within 0.05 rad
Identification of competing disturbing signals	small eccentricity e < 0.03	Grounding, equipotential surfaces		
Temperature stability over measurement interval	Sun-synchronous dawn-dusk orbit (local time of ascending node = sun longitude $\pm$ 90°)	Test Mass temperature stability of 0.1 °/day		
Rejection of disturbing accelerations in MBW	$>$ 600 km perigee, driven by air drag magnitude	drag-free control		
Rejection of disturbing acceleration, any frequency		TM Grounding. Magnetic moment of each TM $< 1 \cdot 10^{-7}\ Am^2$. Magnetic susceptibility of each TM $< 1 \cdot 10^{-6}$		
Data collection and transmission		Assumed antenna: LGA, hemi-coverage. No real time data transmission S-band TT&C Downlink data rate: $<$ 1Mbits/s. Power available for comm (Watts): 20	Data volume per day: 2.4 Gbit. 4 x 10 min passes per day. Spacecraft data destination: MOC. Science data destination : SOC.	
Experiment resources		Mass: 80 kg. Power: 60 W. Volume: 0.2 m^3. Data Rate: 12 kbit/s. Temperature range: ambient.	Bit error rate $< 1 \cdot 10^{-5}$. Tune correlation to 2 msec over 1 week	
Spacecraft resources		Mass: 400 kg. Power: 300 W. Volume: 3.5 m^3. Data Rate: 30 kbit/s. Ambient Temp		

Table 8: Microthrusters requirements

Maximum thrust	$\geq 150\ \mu N$	50% margin
Max thruster response time	40 ms	@ commanded step (up and down) $\geq 60\ \mu N$
Resolution (quantization)	$24\ \mu N$	TBC, not critical
Max noise	$18\mu N/\sqrt{Hz}$	Around 1 Hz
Scale factor error	12%	Peak
Update com rate	10 Hz	TBC
Total impulse	4500 Ns	20% margin
Minimum thrust	$\leq 10\mu N$	TBC
Vector stability	0.17 rad	Peak, at $60\mu N$
Centrifugal acceleration	$<$ 4.4 g	20 % margin, 0.75 m s/c radius

The driving thermal control requirements include: test mass mean temperature stability better than 0.1° C/day; axial temperature gradient of the proof masses shall not exceed 1° C/arm length; temperature fluctuations in the proof masses shall not exceed 0.2° C in 1 day; linear temperature drift in the proof masses shall not exceed 0.2°C/day.

Preliminary finite element and thermal math models are available (tailored to a different launcher) and may be readily adapted to study the accommodation in VEGA.

The experiment resources are modest and undemanding for both the satellite and the ground segment. The most challenging system requirements are related to the drag-free control. Micro-Newton thrusters, producing finely tuned forces (in magnitude and frequency), are fundamental to achieving the objectives of the EP experiment, and a design driver of the spacecraft configuration. The microthruster requirements are summarized in Table 8. These requirements are in the scope of the GAIA cold-gas microthrusters.

After launcher separation, the Drag-Free and Attitude Control System (DFACS) provides spacecraft attitude control and spin-up to the required spin rate of 1 Hz. Thereafter, the PGB is unlocked and the microthrusters are enabled. From then on, the DFACS provides drag compensation with very high rejection ratio, as well as whirl control and control of the spacecraft spin rate and of the PGB-spacecraft relative rotation rate, necessary for maintaining the integrity of the PGB suspensions.

Table 9: Satellite mass and power budgets (from 2009 ASI study, modified to reflect sun synchronous orbit and cold-gas micropropulsion)

Module	**Subsystem or unit**	**CBE Mass [kg]**	**Mass Margin**	**CBE + Mass Margin [kg]**	**Power [W]**
Payload Module					
	Test Masses	20.0	0%	20.0	
	PGB equipped	27.2	20%	32.6	
	Experiment Control Electronics	4.5	20%	5.4	10.8
	Control & Processing Electronics	6.0	20%	7.2	21.6
Service Module					
	Structure	102.1	20%	122.5	
	Thermal Control	8.7	20%	10.4	14.4
	Communications	9.6	10%	10.6	27.8
	Data Handling	16.0	20%	19.2	19.8
	AOCS	4.0	20%	4.7	10.7
	Propulsion	36.4	10%	40.0	25.5
	Power	32.4	13%	36.6	44.5
	Harness	12.5	20%	15.0	
Spacecraft	**Nominal**			**324.3**	**175.1**
	System margin		20%	64.9	35.0
	Total			**389.2**	**210.1**
	Propellant			10.0	
	Total wet			**399.2**	

The early attitude modes use sun sensors and magnetometer for attitude determination, supplemented with a gyroscope in eclipse and for FDIR, and impulsive cold-gas thrusters as actuators. In the science measurement phase, four independent controllers are active: The XY drag-free controller, for drag compensation in the XY plane: this controller shall reduce the drag disturbances at the spin rate providing a rejection better than $2 \cdot 10^{-5}$; the XY whirl controller, for stabilizing the motion in the XY plane, by a low-frequency action; the Z drag-free controller, for drag compensation and displacement reduction along the Z axis; the spin-axis angular rate controller, to limit the relative rotation between PGB and satellite. The XY drag free controller uses the microthrusters for actuators, in closed loop with the capacitance sensors of the science accelerometers (in common mode). The control of the Z displacement and of the whirl is realized by acting on the capacitance plates. Supplementary sensors include the spin rate sensor, for accurate determination of the fractional spin rate change, and photo-detectors for the phase lag between the PGB and the spacecraft outer shell. The latter control action is actuated by the microthrusters. The XY drag-free controller is the most challenging task, considering the very fine drag compensation required and the limitation on the response time of the available actuators, which reduces the usable command update rate. The DFACS requirements, architecture, algorithms, and the specific technologies have been investigated in detail as part of the ASI Phase A study.

The results from the analysis and simulation show that the proposed solutions meet the requirements with adequate margins, with the available technologies.

6 Science operations and archiving

Table 10 summarizes the mission profile. The mission lifetime is 9 months. 20 days are estimated sufficient for the initial set up and calibration; 250 days are available for the scientific mission. During this time interval, two attitude manoeuvres are performed for spin axis alignment, each estimated to take 10 days including rebalancing of the experiment. 230 days are left for science measurements, i.e. 3 intervals of 1140 orbits each (orbit period = 5800 s).

15 orbits suffice for one measurement to $\eta = 10^{-17}$ (low thermal noise; discrimination of effects at close-by frequencies). Such measurements must be passive, with no whirl control on. Every 100 orbits (Q=20000), whirl amplitude is quickly brought to zero by the capacitive sensors/actuators. In 76 days 76 measurements of the weak EP to 10^{-17} are carried out. During these measurements the angle between spin axis and orbit normal changes from -38^{o} to $+38^{o}$, which provides ample room for discriminating quadrupole mass coupling and tidal and magnetic effects. The procedure is repeated 3 times, providing multiple redundancy of the measurements. Any interruptions are tolerated simply by suspending the science measurements and waiting for spacecraft health to be

Table 10: GG Mission phases

Mission elapsed time (days)	Phase	Tasks
0 – 20	Commissioning/ Calibration	S/C commissioning. Experiment setup and calibration
20 – 97	First measurement phase	76 x 15-orbit EP measurement intervals with whirl control off. Whirl control activation once in 100 orbits
97 -107	Reorientation phase	Reorientation manoeuvre by on-off N2 thrusters. Experiment re-balancing
107 – 183	2^{nd} measurement phase	76 x 15-orbit EP measurement intervals with whirl control off. Whirl control activation once in 100 orbits.
183 – 193	Reorientation phase	Reorientation manoeuvre by on-off N2 thrusters. Experiment re-balancing
193 – 270	3^{rd} measurement phase	76 x 15-orbit EP measurement intervals with whirl control off. Whirl control activation once in 100 orbits.

restored, with little effect on the overall mission performance.

At least two independent teams shall be in charge of processing the raw data. The two teams shall work independently and provide independent analyses of the raw data. They shall agree on common standards for the preprocessing (same set of universal constants, etc.) and the GG orbit determination shall be agreed or computed in cooperation. Instead, the data processing algorithms shall be completely independent. Each team shall be required to provide the output of its data processing together to the description of the adopted reference systems, kinematics, dynamics, observable handling, observation equations, etc. The output of the two teams shall be finally shared and compared in order to address the science output of the mission.

One of the data processing teams will be located at the PI's Institute, the other may be organised by ESA or another cooperation partner. ASI will fund the science operations and archiving. After publication of the experiment results, the whole data base will be made publicly available.

7 Development schedule and technology readiness

As shown in Fig. 14 GG fits a 4-yr implementation timeline with start of Phase B in late 2013, 3-yr Phase C/D and launch within 2017.

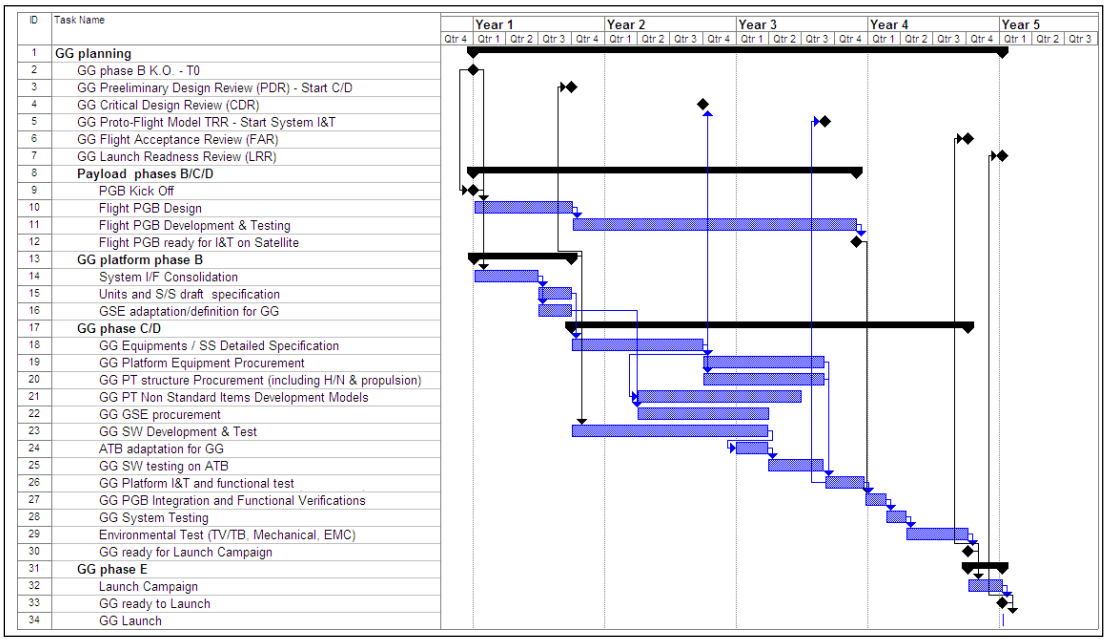

Figure 14: GG implementation schedule (taken from 2009 ASI study)

At the satellite system level, a Proto Flight Model (PFM) approach is envisaged. Prior to the PFM programme, the satellite functional performances will be validated using a dedicated End to End simulator (purely SW) plus an Avionics Test Bench where representative HW will

Table 11: GG payload development models

Item	DM/STM	EQM	FM
PGB mechanics (flexures)	1 DM		Included in PGB
PGB Assembly	1 STM		1 PFM
PGB lock mechanism			Included in PGB
TM lock mechanism	1 DM 1 STM		Included in PGB
Inner Test Mass	1 STM		1 PFM
Outer Test mass	1 STM		1PFM
ECE	dummy	1 EQM	1 PFM

be incrementally included in the loop, whereas the satellite-level thermo-structural performances and compliance with the relevant requirements will be evaluated by analysis. The PFM will be the final product after integration, and the item that will be launched. It will be subjected to a complete proto-flight test campaign in order to confirm the functional validation performed on simulators, and the thermo-structural performances will be evaluated by analysis.

All platform equipment have flight heritage or are derived from equipment with flight heritage, with one exception, the spin rate sensor (Fig. 15). The envisaged sensor consists of a small telescope with Position Sensing Detector (PSD) for measuring the optical power and the coordinates of the light spot focused on the focal plane (figure). A prototype of this rate sensor was designed, a performance model was prepared, and the breadboard was manufactured and successfully tested within the 2009 GG Phase A2 study for ASI. There is no new technology involved, and the sensor meets the requirements for TRL5.

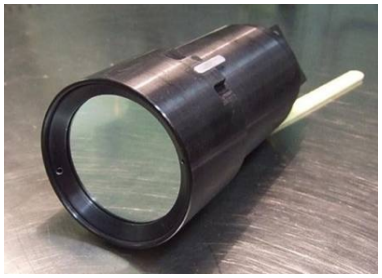

Figure 15: Fully integrated spin rate sensor breadboard (realized within 2009 ASI study)

The drag free control heritage from GOCE, and relevant for GG, includes the design and development approach based on an end-to-end simulator, and the design, development, test and in-flight verification of the drag-free control. In addition, the experience of GOCE is relevant to the management of a sensitive experiment whose in-flight performance objective was 3 orders of magnitude away from the performance that could be verified on the ground. The GAIA cold-gas microthrusters, soon to be verified in flight, were qualified in 2010 and are therefore TRL8.

As for the payload, the existing GGG experiment will be used as a demonstrator model, in terms of both specific design and test issues. The GGG test equipment will be assessed for upgrading and use for functional testing of the GG space accelerometer. The main assembles of the instrument are the Pico-Gravity-Box (PGB) and two electronic units, the Control and Processing Electronics (CPE), mounted on the spacecraft, and Experiment Control Electronics (ECE), mounted inside the PGB.

Neither mechanics nor electronics require substantial technology development, given the experience from the ground experiment. Development models are envisaged for the PGB mechanics (for form-and-fit) and 0g flexures; the wireless data transmission, and the lock mechanisms.

Structural Thermal Models (STM) of the test masses and PGB shell will be manufactured early in the program to confirm that the interface is correctly matched. The masses will be used in the STM instrument for thermal/mechanical testing. For the wireless data transmission an engineering model will be developed and validated by implementing it in the GGG instrument. For the launch locks, a breadboard will be developed of one set of mechanisms and the related electronics (as necessary to control one mechanism).

The proposal baseline is test mass displacement readout by capacitance sensors. The capacitance readout system is a state of the art application with no development issues. This readout will be replaced by a laser gauge readout if JPL joins the mission. Building qualification models of the laser metrology system is seen as unnecessary based on JPL prior experience with building similar hardware. The lasers are flight spares from a mission that has been on orbit several years (TES) and are TRL 9. The beam launchers are closely based on beam launchers brought to TRL 5/6 for SIM and other programs. The fibre optics are similar (fibre/jacket/connector) to other fibre optics that have been qualified and/or flown on other programs (LOLA, MSL, others) and should be qualified at a higher level of assembly than the fibre. PFM lasers and beam launchers with spares will be built and shipped to Europe for integration to the FM PGB and flight acceptance testing. Environmental testing on the PFM instrument (vibration, thermal vacuum) will be done as part of the system PFM program.

8 Proposed implementation scheme and cost

The proposed mission is implemented in 4 years, from Phase B to launch (see Fig. 14) and has a required in-orbit lifetime of 9 months. The spacecraft is launched by VEGA into a standard near circular sun-synchronous orbit at an altitude of $\simeq 600$ km, using the full lower compartment (VESPA) in a dual-launch configuration. The spacecraft is an ad-hoc structure, for the reasons mentioned in Sec. 5, endowed with equipment of standard design. The payload is accommodated in a dedicated module, the PGB, allowing parallel developments till late in the AIT cycle. The proposed model approach is protoflight, with development models of some payload elements relying on the existing ground experiment for risk mitigation.

The design of the spacecraft and payload has heritage in two Phase A studies performed in recent years by Thales Alenia Space Italy for ASI. The relevant materials are partially published in the PI's web site ([31] [32] [33]). ASI will take care to make the full set of documents available to ESA should GG be selected or should it be relevant in the selection process.

Given this heritage, the following responsibilities are proposed (Table 12):

- ASI will act as mission architect and provide the science payload and operations
- ESA will act as spacecraft architect, procure the spacecraft platform and equipment, and provide the launch.

This work breakdown is logical and appropriate and it is suitable for simple management interfaces between the two major partners.

Since 2010 there exists a collaboration on GG between the PI's Institute and the Jet Propulsion Laboratory (JPL) of NASA with Dr. Michael Shao as JPL team leader. So far, this collaboration, which has already produced a number of joint papers published in high-profile journals, had centred on the intention to submit a proposal to the next EXPLORER call of NASA, expected in 2013. With the opening by ESA of this Call for a small mission, in the event of GG being selected, JPL to seek NASA funding of a part of the GG payload within the NASA Call for a Mission of Opportunity expected this fall. In particular, JPL's Division of Instrument and Science Data Systems would produce the precision test masses and the Laser Metrology subsystems for the instrument. JPL's Laser Gauge readout would replace the cap gauge readout taken as baseline in this proposal. JPL's provision would base on the qualified metrology architecture for the Space Interferometry Mission (SIM). In order to capitalize on its investment on GG, and to take advantage of the opportunity opened by ESA, ASI will encourage and manage the collaboration of JPL and will seek the participation of other European agencies.

The development of GG was the subject of a cost estimating exercise at the end of the ASI 2009 Phase A-2 study. The following remarks apply to the 2009 cost estimate and, given the similarity of the provisions stipulated then and now, to the 2012 cost estimate for ESA as well.

The cost estimating exercise was carried out by the Cost Analysis team belonging to the Contract & Proposals Unit of the Sales Dept. of TAS-I BU OOS, in collaboration with the GG Phase A engineering team.

Table 12: Work breakdown and corresponding responsibility

Role	Responsibility description	Funding Agency	Implementation
Mission Architect	Overall mission execution. Mission-level requirements for meeting the science objectives. Mission reference concept. Mission performance in orbit.	ASI	ASI
Spacecraft Launch	Launcher Procurement. Spacecraft transportation to the launch site and launch campaign.	ESA	ESA
Spacecraft Architect	Spacecraft system and subsystems requirements, system engineering and technical performance. Assembly, integration and verification at system level.	ESA	ESA + Industry
Spacecraft Platform	Design, development and verification of the spacecraft platform.	ESA	Industry
Science Payload	Design, development and verification of the science instruments.	ASI	PI
Mission Operations	Spacecraft tracking, telecommand and telemetry during the lifetime in orbit, including de-orbiting at end of life if required.	ESA	ASI
Science Operations	Scientific mission planning in orbit, science data processing, distribution and archiving.	ASI	ASI

The method utilized for the definition of the forecast production cost is based on a bottom-up identification of the effort (in term of manpower costs and other costs - travels, materials, etc) necessary to accomplish the planned activities. The entry point is the program schedule where all the activities, organized as per Work Breakdown Structure, are foreseen and detailed. The sources of the estimates are the Business Units (BU) and Industrial Units (IU) of TAS-I, plus a selected number of external companies who, on request, provided cost estimates of specific items. The cost exercise was carried out over a time period of more than 2 months, and it involved all the Business Units and Industrial Units of TAS-I that would actually be involved in Phase B/C/D/E. The manpower estimates were refined over a number of fact-finding and review meetings. The equipment and materials costs were based on price quotations obtained in the course of the most recent company programs, no quotation being older than about 1 year. Whenever the implementations required for GG were understood to deviate from the current state of the art, Requests for Information were sent to the most reliable manufacturers of that specific field, who were then involved in technical discussions until a clear cost baseline was agreed.

The exercise addressed not only engineering, procurement and integration and test activities, but also manufacturing, raw materials, ground support equipment, transportation, and insurance. Finally, the ROM (Rough Oreder of Magnitude) price included an allowance for project risk, estimated from a dedicated risk analysis exercise. The cost estimate was subjected to the standard review cycle for such projects, including a final review by the Company's upper management.

The cost table provided to ESA (Table 13 of the proposal, not reported in the present text) includes adjustments for the changed economic conditions (escalation from mid-2009 conditions to mid-2012 conditions at a European-average 3-year cumulative inflation rate of 5.45%), launch, launch services, ground and science operations which were not included in the 2009 cost estimate. In addition, the cost estimate of the Micropropulsion has been updated (FEEP was the 2009 baseline and is now replaced by cold-gas proportional thrusters).

The resulting total cost in 85 M€.

9 Communication and outreach

A space mission to investigate the foundations of gravity has great outreach potential. Galileo, Newton and Einstein embody the very idea of the scientist in the public imagination. The concept of the universality of free fall may seem natural and unproblematic, until the story is told of how long it took to establish it, and of the puzzle it continues to represent for contemporary science, once the equivalence of mass and energy enters the picture. General Relativity theory is conceptually subtle, but the ideas it rests on, first among them the universality of free fall, are not difficult to explain, and it has made headlines all through its history, from Eddington's 1919 eclipse expedition to Fishbach's 1986 "fifth force" paper in the front page of the New York Times. The experimental side of the UFF, from simple mass dropping to the pendulum, the torsion balance and the innovative idea GG rests on, lends itself well to explaining the slow and meticulous way science progresses; and the fact that, at the end of the day, experiment, hence nature, decides, is an important lesson for interested and curious laymen as well as for physicists.

The physics of the GG experiment has many facets that lend themselves for use in the classroom at all levels, from basic lab demonstrations in secondary school to advanced engineering and physics courses at university level. For years GG has been used at the University of Pisa as a source of real world problems for physics students; it has been the subject of many newspaper articles and it has featured in local and national TV and radio shows. Public talks about gravity and GG have featured in science festivals around Italy, never failing to attract interested audiences. On visiting a police station after being the victim of street theft, the PI was astonished to hear the policeman in charge asking, after learning she was a physicist, about the current status of testing relativity!

The outreach potential of GG will be developed using both traditional and unconventional media. Presence on the internet will be expanded via dedicated web sites, Wikipedia entries. You Tube can host animations as well as video recordings of talks, lessons and demonstrations. Social media (facebook, twitter) can be employed to build up a community of followers. To raise the level of awareness of the general public, events (public talks, exhibitions) will be organized and press releases will be used on the occasion of important project milestones. On the educational side, specialized literature will be developed for teachers and students at primary - secondary - university level. Science has a duty to be accountable and report to the citizens that support it, and GG has plenty of materials and ideas to educate and inspire the public, and let it have fun too.

References

[1] C. M. Will, Living Rev. Relativity, 9, 3 (2006) http://relativity.livingreviews.org/Articles/lrr-2006-3
[2] Y. A. Ono Physics Today 35(8), 45 (1982)
[3] A. Einstein, *Relativitätsprinzip und die aus demselben gezogenen Folgerungen*, Jahrbuch für Radioaktivität und Elektronik, 4, 411-462 (1907); *On the relativity principle and conclusions drawn from it*, in H. M. Schwarz, *Einstein's comprehensive 1907 essay on relativity, part III*, American Journal of Physics, 45 (10) 899-902 (1977)
[4] A. Einstein *Grundlage der allgemeinen Relativitätstheorie*, Annalen der Physik (ser. 4), 49, 769-822 (1916); *The Foundation of the General Theory of Relativity*, in *The Principle of Relativity*, Dovrer Pub. Inc. N.Y., USA (1952)
[5] R. V. Eötvös, D. Pekar, E. Fekete, Ann. Phys. 68, 11-66 (1922)
[6] P. G. Roll, R. Krotkov, R. H. Dicke, Ann. Phys. 26, 442-517 (1964)
[7] V. B. Braginsky, V. I. Panov, Sov. Phys. JEPT 34, 463-466 (1972)
[8] S. Baeßler *et. al.,* Phys. Rev. Lett. 83, 3585 (1999)
[9] S. Schlamminger *et. al.,* Phys. Rev. Lett. 100, 041101 (2008)
[10] S. Fray *et. al.*, Phys. Rev. Lett. 93, 240404 (2004)
[11] A. Peters, K. Y. Chung, S. A. Chu, Nature 400, 849 (1999)
[12] J. G. Williams, S. G. Turyshev & D. H. Boggs, Phys. Rev. Lett. 93, 261101 (2004)
[13] J. Mueller, F. Hoffman & L. Biskupek, *Testing various facets of the equivalence principle with Lunar Laser Ranging*, Class. Quantum Grav. focus issue on the WEP, to appear
[14] E. G. Adelberger *et al.,* Progress in Particle and Nuclear Physics 62, 102 (2009)
[15] T. W. Murphy *et al.*, Icarus 211, 1103–08 (2011)
[16] A. M. Nobili *et al.*, General Relativity & Gravitation 40, 1533-1554 (2008)
[17] R. Pegna *et al.*, Phys. Rev. Lett. 107, 200801 (2011)
[18] T. J. Quinn, C. C. Speake, R. S. Davis, Metrologia 23, 87-100 (1986)
[19] P. Touboul, Space Sci. Rev. 148, 455-474 (2009)
[20] Nobili *et al.*, *"Galileo Galilei" (GG): space test of the weak Equivalence Principle to* 10^{-17} *and laboratory demonstrations*, Class. Quantum Grav. focus issue on the WEP, to appear
[21] R. Pegna *et al.*, *Integration time of high sensitive equivalence principle experiments in space,* to be submitted
[22] P. Touboul and M. Rodrigues, Class. Quantum Grav. 18, 2487-2498 (2001)
[23] J. P. Blaser *et al. Satellite Test of the Equivalence Principle*, Report on the Phase A Study, ESA/NASA SCI (93)4 (1993)
[24] J. P. Blaser *et al. Satellite Test of the Equivalence Principle*, Report on the Phase A Study, ESA SCI (96)5 (1996)
[25] L. I. Schiff, AJP 28, 340 (1960)
[26] A. M. Nobili *et al.*, *On the universality of free fall, the equivalence principle and gravitational redshift,* to be submitted
[27] G. Holton *Thematic origins of scientific thought*, Harvard Univ. Press (1973)
[28] A. M. Nobili *et al.*, Phys. Rev. D Rapid Commun. 63, 101101(R) (2001)
[29] A. M. Nobili *et al.*, New Astronomy 7, 521-529 (2002)
[30] G. L. Comandi *et al.*, Phys. Lett. A 318, 213-222 (2003)
[31] A.M. Nobili *et al.*, *GG Mission Studies, ASI* http://eotvos.dm.unipi.it/documents/missionstudies
[32] A.M. Nobili *et al.*, *GG Phase A Study, ASI* (1998) http://eotvos.dm.unipi.it/ggweb/phaseA
[33] A.M. Nobili *et al.*, *GG Phase A-2 Study, ASI* (2009) http://eotvos.dm.unipi.it/PA2/GGPhaseA2StudyReport2009.pdf